HHS Public Access

Author manuscript

Biochim Biophys Acta Mol Basis Dis. Author manuscript; available in PMC 2019 October 01.

Published in final edited form as:

Biochim Biophys Acta Mol Basis Dis. 2018 October ; 1864(10): 3353–3367. doi:10.1016/j.bbadis.2018.07.022.

Aberrant cardiolipin metabolism is associated with cognitive deficiency and hippocampal alteration in tafazzin knockdown mice

Laura K. Cole[1,2], **Jin Hee Kim**[1,3], **Andrew A. Amoscato**[4], **Yulia Y. Tyurina**[4], **Hülya Bayır**[5], **Benyamin Karimi**[2,3,6], **Tabrez J. Siddiqui**[2,3,6], **Valerian E. Kagan**[4], **Grant M. Hatch**[1,2,7,*], and **Tiina M. Kauppinen**[1,2,3,*]

[1]Department of Pharmacology & Therapeutics, Faculty of Health Sciences, University of Manitoba, 753 McDermot Avenue, Winnipeg, MB R3E OW3, Canada.

[2]The Children's Hospital Research Institute of Manitoba, Winnipeg, MB, Canada

[3]Neuroscience Research Program, Kleysen Institute for Advanced Medicine, Health Sciences Center, Winnipeg, MB R3E 0Z3, Canada.

[4]Center for Free Radical and Antioxidant Health, Department of Environmental and Occupational Health, University of Pittsburgh, Pittsburgh, PA, USA.

[5]Safar Center for Resuscitation Research, Children's Hospital of Pittsburgh, Department of Critical Care Medicine, University of Pittsburgh, Pittsburgh, PA, USA.

[6]Department of Physiology & Pathophysiology, Faculty of Health Sciences, University of Manitoba, 753 McDermot Avenue, Winnipeg, MB R3E OW3, Canada.

[7]DREAM, The Children's Hospital Research Institute of Manitoba, Biochemistry and Medical Genetics, Center for Research and Treatment of Atherosclerosis, University of Manitoba, Winnipeg, MB, R3E 0T6, Canada

Abstract

Cardiolipin (CL) is a key mitochondrial phospholipid essential for mitochondrial energy production. CL is remodeled from monolysocardiolipin (MLCL) by the enzyme tafazzin (TAZ). Loss-of-function mutations in the gene which encodes *TAZ* results in a rare X-linked disorder called Barth Syndrome (BTHS). The mutated TAZ is unable to maintain the physiological CL:MLCL ratio, thus reducing CL levels and affecting mitochondrial function. BTHS is best known as a cardiac disease, but has been acknowledged as a multi-syndrome disorder, including cognitive deficits. Since reduced CL levels has also been reported in numerous neurodegenerative

*Corresponding authors: Tiina M. Kauppinen, Ph.D., Tiina.Kauppinen@umanitoba.ca Tel: (204) 789 3846, Grant M. Hatch, Ph.D., ghatch@chrim.ca. Tel: (204) 789 3405.

Author contributions

L.K.C, J.Y.H., A.A.A., Y.Y.T., H.B., V.E.K., B.K., T.J.S. performed experiments and interpreted results. G.M.H. and T.M.K. were responsible for conceptual design. L.K.C., T.M.K. and G.M.H. wrote the initial draft. L.K.C., H.B., V.E.K., G.M.H. and T.M.K. edited the manuscript. G.M.H. and T.M.K. gave final approval and agreed to be accountable for all aspects of work ensuring integrity and accuracy.

Conflict of Interest

The authors have no conflict of interest.

disorders, we examined how TAZ-deficiency impacts cognitive abilities, brain mitochondrial respiration and the function of hippocampal neurons and glia in TAZ knockdown (TAZ kd) mice. We have identified for the first time the profile of changes that occur in brain phospholipid content and composition of TAZ kd mice. The brain of TAZ kd mice exhibited reduced TAZ protein expression, reduced total CL levels and a 19-fold accumulation of MLCL compared to wild-type littermate controls. TAZ kd brain exhibited a markedly distinct profile of CL and MLCL molecular species. In mitochondria, the activity of complex I was significantly elevated in the monomeric and supercomplex forms with TAZ-deficiency. This corresponded with elevated mitochondrial state I respiration and attenuated spare capacity. Furthermore, the production of reactive oxygen species was significantly elevated in TAZ kd brain mitochondria. While motor function remained normal in TAZ kd mice, they showed significant memory deficiency based on novel object recognition test. These results correlated with reduced synaptophysin protein levels and derangement of the neuronal CA1 layer in hippocampus. Finally, TAZ kd mice had elevated activation of brain immune cells, microglia compared to littermate controls. Collectively, our findings demonstrate that TAZ-mediated remodeling of CL contributes significantly to the expansive distribution of CL molecular species in the brain, plays a key role in mitochondria respiratory activity, maintains normal cognitive function, and identifies the hippocampus as a potential therapeutic target for BTHS.

Keywords

cardiolipin; monolysocardiolipin; tafazzin; Barth Syndrome; brain; hippocampus; cognition

Introduction

Cardiolipin (CL) is considered the signature phospholipid of the mitochondria because it is both synthesized and localized exclusively within this organelle[1]. The role of CL in the mitochondria extends from maintaining membrane fluidity to an intimate association with bioenergetic processes. It is well-established that CL promotes the structural and functional integrity of individual respiratory chain enzymes, substrate carriers and the assembly of mitochondrial supercomplexes. For example, removal of CL from respiratory chain proteins results in denaturation and complete loss of activity which cannot be effectively substituted with other phospholipids[2–6].

The appropriate fatty acid composition of CL is also crucial for maintaining normal mitochondrial function. Immediately following *de novo* synthesis, the acyl chains are rapidly remodelled to generate a specific pattern of mature CL molecular species. In most mammalian tissues the predominant form of this unique tetra-acyl phospholipid consists entirely of linoleic acyl chains (L_4-CL, 40–80%). The fatty acid composition of CL significantly affects the activity of mitochondrial membrane proteins and the efficiency of oxidative phosphorylation[7–9].

It is clear that taffazin (Taz) plays a central role in generating the appropriate composition of mature CL species. Tafazzin is an X-linked mitochondrial transacylase that transfers fatty acyl groups from glycerophospholipids to monolysocardiolipin (MLCL)[10–13]. The

importance of TAZ in maintaining CL levels and mitochondrial function is well-established. For example, cells deficient in TAZ have reduced CL content, alteration in molecular CL species and mitochondrial dysfunction all of which can be restored when TAZ is reintroduced[14–17]. Furthermore, loss-of-function mutations in *TAZ* results in the rare genetic disorder Barth Syndrome (BTHS)[18]. The common clinical features of BTHS, cardiomyopathy and skeletal muscle weakness, have been attributed to loss of CL content and deficiencies in the mitochondrial respiratory enzymes which lead to reduced oxidative phosphorylation[3,19].

Emerging evidence now supports the role of CL in maintaining normal metabolic function and viability of the brain[20]. CL comprises approximately 2% of the phospholipid mass of the whole brain and up to 5.7% of the phospholipid mass in neurons and glial cells[1]. In contrast to the dominant L_4-CL species found in the periphery, more than one hundred different molecular species of CL have been reported throughout the brain[21]. Modification in the species of CL and/or the decrease in its total amount can result in enlarged or dysfunctional mitochondrial. Moreover, reduced/modified CL has been linked to pathogenesis of various neurodegenerative diseases including Alzheimer's disease, Parkinson's disease and the exacerbation of symptoms following traumatic brain injury[21–27].

It has also been demonstrated that BTHS boys commonly exhibit learning difficulty and attention deficits[28–31]. Kindergarten or first-grade boys with BTHS all had significantly lower visual spatial skills, when compared with neurotypical boys of similar age or grade level. Specific aspects of visual short-term memory in BTHS boys also differed from the norm. Mathematical difficulties in boys with BTHS emerged by kindergarten which was proposed to underling changes in executive brain function[31]. As a result of these studies, management of the cognitive profile of BTHS now warrants educational support during the early school-age years[32].

Despite the link between sufficient CL levels and normal brain function it remains unclear whether altered CL in the brain results in cognitive dysfunction. Thus, we investigated whether CL was reduced and/or modified in the brain of tafazzin knockdown (TAZ kd) mice, and if this altered mitochondrial respiration and cognitive function. We demonstrate the profile of changes that occur in brain phospholipid content and composition in TAZ kd brain. This result corresponded with elevated activity of complex I mediated mitochondrial state I respiration, attenuated mitochondrial spare capacity and increased production of reactive oxygen species (ROS) in TAZ kd brain. Because the hippocampus contributes to learning and memory[33], we analysed hippocampal neurons, synapses and glial cells for elevated markers of stress and degeneration. Our results indicate that TAZ kd mice exhibit significant memory deficits and this correlates with reduced synaptophysin protein content and derangement of the neuronal CA1 layer in hippocampus.

Results

Tafazzin deficiency alters the molecular species composition of cardiolipin in mouse brain

The knock-down of TAZ was induced in transgenic (Tg) male mice with the addition of doxycycline (dox) to the rodent diet. We confirmed that the expression of TAZ protein was

reduced in the brain of TAZ kd mice (Tg +dox) mice compared to the dox-fed non-transgenic littermate controls (NTg +dox) as well as the animals fed the standard rodent diet (NTg -dox) (Fig. 1A, B). Subsequent analysis focused on how TAZ kd altered phospholipid levels in the whole brain (Fig.1 C, D). As expected, we determined that TAZ-deficiency resulted in a significant decrease in brain CL (11.34±0.26 pmol/nmol PL) content compared to littermate controls (12.54±0.46 pmol/nmol PL, NTg +dox) (Fig. 1D). With the exception of phosphatidylserine (PS), all phospholipids increased in the brain of TAZ kd mice (Fig 1D). Phosphatidylglycerol (PG) was increased by the largest amount (~38%) in TAZ-deficiency (Tg+dox). A significant accumulation of PG also occurred simultaneously with the loss of CL in the heart of Taz kd (Tg +dox) animals compared to the litter-mate controls (NTg+dox) (Fig 1E, F). We determined that hepatic CL and PG content remained normal in TAZ kd mice which is consistent with our previous findings (Fig 1E, F)[34]. Thus, PG only accumulated when CL levels were also reduced[35]. Analysis of mRNA levels indicated significant reductions in CL synthesis and remodelling enzymes in the brain of TAZ kd (Tg +dox) mice compared to controls (Fig. 1G). The larger reduction in CLS (47%) mRNA levels compared to the other CL biosynthetic genes (~30%) is consistent with an accumulation of PG.

To further examine how TAZ-deficiency alters CL in the brain we quantitated individual molecular species by mass spectrometry (Fig. 2A–C). We determined that total CL was significantly decreased in the TAZ kd mice primarily due to decreases in species (20–80%) most prevalent in long-chain polyunsaturated fatty acids (PUFA) (22:6, 22:5 and 22:4) corresponding to *m/z* 1518 to 1574. This is in contrast to the skeletal and cardiac muscle of TAZ kd mice where the reduction in total CL was primarily due a decrease (~80%) in L_4-CL (1448 m/z) which is the major species comprising 60% of total CL content in these tissues[34]. Overall the content of *m/z* 1448 in wild-type (NTg +dox) brain was unremarkable at ~1.5% of total CL and was modestly elevated in TAZ-deficiency (Fig. 2A). The major species in wild-type mouse brain (NTg +dox) was *m/z* 1478 $((18:1))_3/20:4$) despite only amounting to 6.7% of total brain CL. TAZ-deficiency did result in a significant reduction (~16%) in *m/z* 1478 and the emergence of a replacement dominant species *m/z* 1500 $((18:2)_2/(20:4)_2$ and $(18:0)_1/(18:2)_2/(22:6)_1$). A number of CL species were also significantly increased in TAZ-deficiency with the majority (~65%) having a low molecular weight (<1458 *m/z*) consistent with shorter length fatty acyl chains (≤18 carbons). For example, the largest TAZ kd mediated increases in CL molecular species were in 1404 and 1406 *m/z* (Fig. 2A, 423% and 1281% respectively) which are enriched in fatty acids 18:0/18:1 and 16:0/16:1. Thus, TAZ-mediated remodelling of CL contributes significantly to the expansive distribution of CL molecular species in the brain, particularly those containing one or more long-chain PUFA. In addition, this study is the first to report the extensive changes that occur in the CL molecular species of TAZ kd mouse brain.

Brain lysophospholipid levels are altered in tafazzin knockdown mice

One of the hallmarks of TAZ deficiency in both BTHS patients and animal models is the dramatic accumulation of MLCL. Therefore, we measured brain lysophospholipid levels[36–38]. As expected, we determined that the amount of MLCL in TAZ kd brain was significantly increased (19-fold) resulting in a corresponding elevation in the MLCL/CL

ratio compared to the littermate controls (NTg+dox) (Fig. 3A–C). TAZ-deficiency promoted MLCL abundance due to a broad increase in all molecular species detected (Fig. 3I). However, the largest increases (> 200 fold) were in species (*m/z* 1140, 1166 and 1168) which are enriched with 16:0/16:1 and 18:0/18:1 fatty acids and represent the deacylation products of newly synthesized nascent CL (Fig. 3I).

TAZ is a transacylase which harvests acyl chains from glycerophospholipids to mediate reacylation of MLCL. Analysis of lysophospholipids levels in the brain revealed that total lysophospholipid levels remained similar between the TAZ-deficient animals (Tg+dox, 7.00±0.22 pmol/nmol PL) and the littermate controls (6.78±0.32 pmol/nmol PL). However, the amount of lysophosphatidylglycerol (LPG) was significantly increased and lysophosphatidylcholine (LPC) decreased in TAZ kd mice compared to the control animals (NTg +dox) (Fig. 3A, C). The total amounts of lysophosphatidylserine (LPS), lysophosphatidylinositol (LPI) and lysophosphatidylethanolamine (LPE) were not significantly different between the genotypes despite significant decreases in one or more of the individual molecular species detected (Fig. 3D–H). These data indicate that the lack of TAZ in the brain profoundly affects the molecular composition of CL and phospholipid species which are critical in the maintenance of tissue specific membrane structure and function.

Mitochondrial spare respiratory capacity is attenuated in the brain of Taz kd mice

It is established that reductions in total CL and/or L_4-CL levels are associated with mitochondrial respiratory chain dysfunction[39]. To determine whether TAZ-deficiency also impairs mitochondrial respiration in the brain we measured the oxygen consumption rate (OCR). Oxidative phosphorylation begins with the transfer of electrons to complex I (NADH-Coenzyme Q reductase) or to complex II (succinate-CoQ reductase). Thus, we measured respiration through each pathway. For complex I mediated respiration the state I OCR level (basal respiration in the absence of ADP) was elevated by 160% in mitochondria isolated from the brain of TAZ kd animals compared to the NTg +dox controls (Fig. 4A). The state III respiration level (maximum respiration, when ADP is no longer rate-limiting) was not significantly increased by either the addition of ADP or a respiration uncoupler (FCCP) with TAZ-deficiency (Fig. 4A). Thus, the spare capacity of TAZ kd (Tg +dox) mitochondria was significantly reduced (~50%, Fig. 4B) compared to the littermate controls (NTg +dox). This indicates that TAZ-deficiency compromises mitochondrial respiration in the brain by attenuating the response of complex I to demanding metabolic states. In contrast, complex II mediated OCR was similar between the genotypes for all respiratory states measured (Fig. 4C, D).

Tafazzin-deficiency promotes elevated supercomplex formation in the brain

One way that mitochondrial respiration is regulated is through the assembly of individual electron transport chain complexes into supercomplexes. They are typically comprised of various stoichmetric combinations of Complex I, Complex III and Complex IV and function to promote efficient electron flow and prevent the generation of ROS[39]. It has also been demonstrated that CL physically binds to individual respiratory complexes and preserves the

stability of supercomplex formation[39]. Thus, we investigated whether impaired respiration in TAZ-deficient brain was due to destabilization of mitochondrial supercomplexes.

Mitochondria isolated from brain were analyzed for supercomplex formation using blue native gel electrophoresis (BNPAGE) (Fig 4E). Supercomplexes were visualized in brain mitochondria from both genotypes with an unexpected elevation in abundance with TAZ-deficiency (65%, Fig 4I). In order to identify the associated individual respiratory complexes, we preformed in-gel activity assays. Consistent with previous reports, the vast majority of complex I activity in the brain was associated with supercomplexes in control mice (NTg+dox) (Fig. 4F)[40]. We determined that both the activity associated with the "free" monomeric form (127%) and with supercomplexes (45%) was significantly increased in TAZ kd mice (Tg+dox) compared to the littermate controls (NTg+dox) (Fig 4F, J). Detection of Complex II by in-gel activity assay was limited to the monomer and consistent with our OCR data; similar in quantity between genotypes (Fig. 4 G, K).

In the brain, complex IV activity is associated with the monomeric form as well as supercomplexes[40]. We determined that TAZ-deficiency significantly increased complex IV activity (~40%) in both forms (Fig. 4H, L) compared to the littermate controls (NTg+dox). Furthermore, supercomplexes with elevated CIV activity were primarily associated with higher CI activity which is consistent with CI, CIII, CIV_n complex formation. These results indicate that neither the reduction in CL content nor alteration in molecular CL species was sufficient to destabilize supercomplex formation in the brain of TAZ kd mice. Alternatively, the elevation in CI/CIV containing supercomplexes may promote the observed increase in complex I mediated state I respiration.

Tafazzin kd mice have normal ATP levels and elevated ROS production in the brain

To determine whether the brain of TAZ kd mice maintained normal energy levels we measured ATP levels in brain homogenates. The level of ATP remained consistent between the animal groups suggesting that the CI mediated elevation in OCR and supercomplexes may provide adequate but not addition ATP content in TAZ-deficiency (Fig. 4M). It is established that complex I also significantly contributes to mitochondrial ROS production[39]. This is primarily due to instability of complex I in a monomeric form where electron flow within the complex becomes disrupted and escapes. Consistent with the disproportional elevation in complex I monomeric (127%) vs supercomplexed (45%) forms in TAZ-deficiency, the amount of H_2O_2 was also significantly increased in TAZ kd mice compared to littermate controls (NTg +dox, Fig. 4N).

Mitochondrial structure is preserved in the brain of TAZ-deficient animals

Many tissues obtained from TAZ kd mice and Barth Syndrome patients contain significant mitochondria malformation. The observed morphological alterations include mitochondrial enlargement, reduction in number and the presence of gross structural abnormalities including vacuoles, and concentric layers of cristae[41–44]. We did not observe a detrimental effect of TAZ kd on mitochondrial structures in the brain (Fig. 5A–D). Quantitative analysis of electron micrographs was performed to quantify changes in the morphology of mitochondria in the CA1 region of the dorsal hippocampus. We determined that

mitochondrial density, cross-sectional area and shape were similar between the genotypes (Fig. 5 E–H). The lack of abnormalities was consistent with the relatively small reduction in CL content and maintenance of mitochondrial supercomplex formation in TAZ-deficient mouse brain.

Tafazzin knockdown mice have impaired cognitive function

TAZ-deficiency and/or reduced CL levels has been linked to cognitive deficits therefore, we examined whether the significant changes in brain CL species impacted cognitive function in TAZ kd mice (Tg+dox). The open field test indicated that the locomotor activity of TAZ kd mice was unaffected with similar results for total distance travelled and percent time moving compared to the other mouse groups (Fig. 6A–B). These results clearly indicated that general malaise or lethargy were not confounding factors in our assessment of memory and spatial performance. However, the movement pattern during the open field test suggested that the TAZ kd mice (Tg+dox) experienced greater anxiety. The TAZ-deficient mice spent significantly more time at the edges and less time in the centre of the open field compared to all other genotypes (Fig. 6C–G). Interestingly, we determined that TAZ-deficiency impairs the ability to distinguish a novel object from a familiar one (Fig. 6H, E). In contrast to the mice fed a standard diet (NTg, Tg -dox) and littermate dox-fed controls (NTg +dox), the TAZ kd mice did not have a significant preference for the novel object. Instead the TAZ kd (Tg+dox) mice spent similar lengths of time exploring both objects indicating an inability to remember being previously introduced to the familiar object (Fig. 6I).

Tafazzin knockdown in mice results in CA1 synaptic protein degradation, neuronal derangement and microglial activation

Since the hippocampus contributes to recognition memory, we examined the morphology of hippocampal neurons and glia of TAZ-deficient mice. The hippocampal neurons of TAZ kd mice (Tg+dox) showed reduced protein content of synaptophysin, a presynaptic vesicle protein (Fig. 7A, C). In addition, we observed significant derangement of the hippocampal CA1 neuronal layer in the TAZ deficient animals (Tg +dox) as assessed by of NeuN immunostaining (Fig. 7B). The percentage of densely organized CA1 neurons was reduced in TAZ kd mice compared to all other genotypes (Fig. 7D). This was due to a reduction in the width of tightly organized densely packed neurons combined with an increase in the total width of the CA1 (Fig. 7E, F). The brain immune cells, microglia, showed signs of activation in TAZ kd mice. Microglial number, portion of morphologically activated (transformed towards hypotrophic and amoeboid) and Iba1 protein expression were elevated in the hippocampus of TAZ kd (Tg +dox) mice compared all other groups (Fig. 8A, C). Astrogliosis was not observed upon TAZ knockdown (Fig. 8B, D).

Discussion

Increasing evidence has implicated altered brain CL in the pathologic development of cognitive dysfunction in aging and multiple neurodegenerative disorders including Alzheimer’s disease and Parkinson’s disease[20,27,45,46]. However, a link between CL and cognitive impairment has not been clearly established. The goal of this study was to use the

TAZ kd mouse to examine the brain for changes in both CL content and molecular species as well as assess any associated mitochondrial and cognitive dysfunction.

We determined that TAZ-deficiency in the brain significantly reduced total CL levels, dramatically increased MLCL levels, and extensively transformed the molecular species composition of CL and all lysophospholipid species measured. This is the first study to report the detailed changes in CL and MLCL that occur in the brain of TAZ kd mice and demonstrate that TAZ-mediated remodelling of CL contributes significantly to the expansive distribution of CL molecular species in the brain. We have also demonstrated that TAZ-deficiency in the brain results in altered mitochondrial respiration, elevated ROS production and significant recognition memory deficiency. These results were correspondingly accompanied by neuronal derangement and elevated markers of microglia activation in the hippocampus of TAZ kd animals. The concurrent nature of these alterations in TAZ kd mice emphasizes the critical role of TAZ in mitochondrial metabolism and phospholipid composition in the brain and provides a basis for understanding the role of CL content and remodeling in the development of neuropathology.

CL is essential to maintain normal mitochondrial function including the efficiency of oxidative phosphorylation[7–9]. Neurons are predominately dependent on oxidative metabolism to satisfy the high energy demands of maintaining membrane excitability and to execute neurotransmission[38,46]. The present study demonstrated that TAZ kd in mouse brain significantly reduced CL content (10%) compared to littermate controls. We determined that this corresponded with a significant elevation in complex I mediated basal respiratory rate and attenuated spare respiratory capacity in the TAZ kd mice. Our results are similar to prior measurements of respiratory function in cardiac tissue from TAZ kd mice[48], BTHS iPSC-derived cardiomyocytes[49], and TAZ-deficient lymphocytes[50], where the elevation in basal respiration was a result of excess proton leak. Typically, impaired mitochondrial respiration corresponded with a larger reduction in CL content >60%. Thus, our results indicate that a small CL reduction in the brain is sufficient to impair oxidative phosphorylation and underscores the sensitivity of neurons to mitochondrial dysfunction. While impaired mitochondrial respiration in the brain did not cause a global decrease in ATP, neurons have a complex morphology comprised of dendritic, somatic, axonal and presynaptic segments each of which requires a local energy supply which may not be reflected. Furthermore, in TAZ kd the attenuated spare capacity indicates reduced access to ATP for energy demanding neuronal events which are critical to maintain normal brain function.

In the current study, TAZ deficiency in the brain resulted in reduced CL content and altered distribution of molecular species. The prevailing model is that both CL content and remodeling are critical for optimal mitochondrial function. However, there is accumulating evidence that the molecular species of CL may not be a major contributor in regulating mitochondrial respiration[35,51–53]. In animal models, mitochondrial respiratory dysfunction could neither be induced[51] nor prevented[50] as a result of altering CL acyl chain composition. Similarly, in yeast lacking TAZ, mitochondrial respiration was not rescued when the distribution of CL species was maintained[52]. The authors demonstrated that CL content alone rescued TAZ-mediated mitochondrial respiration dysfunction regardless of acyl chain composition[35].

In BTHS patient and TAZ kd derived tissues, CL deficiency typically affects mitochondrial respiration in conjunction with reductions in supercomplex stability, and/or the presence of gross mitochondrial structural abnormalities[34,43,44,50]. However, TAZ knock-down in cultured cells and yeast have significant respiratory impairments which are not contingent upon disruption of mitochondrial organization or structure[35,49–51]. The interplay between the roles of CL in mitochondrial structure, organization and function remain unclear. There is evidence that the molecular species of CL may be crucial in regulating supercomplex stability[54]. When CL was enriched in various unsaturated fatty acids (oleic, linoleic, or palmitoleic) the abundance of supercomplexes correspondingly increased[54]. The elevated abundance of supercomplexes is proposed to sequester CL from degradation. Thus, extensive supercomplex destabilization and CL degradation are proposed to occur in parallel. This is consistent with our current study where elevated supercomplex stability was accompanied with only a minor reduction in CL content. It is possible that the alteration in CL molecular species in TAZ kd brain may contribute in part to the elevation in supercomplexes despite an overall decrease in long-chain unsaturated fatty acid containing CL species. Alternatively, the increase in total supercomplex content may reflect the differential assembly of supercomplexes in astrocytes and neurons[55].

Currently, it is predicted that the extensive array of CL molecular species (>100) in the brain, particularly those containing PUFA, are involved in neuronal signaling[20,56]. Hydrolysis of CL by phospholipases facilitates mitochondrial dynamic events which may be crucial for neurogenesis and determination of neuronal stem cell fate[47]. Cognitive dysfunctions were previously observed in $iPLA_2$ knockout mice[56]. These mice had extensive alterations in brain CL species with a shift to shorter chain length molecular species. TAZ-deficiency generated similar alterations in brain CL with reduced PUFA-containing species and enrichment in shorter length fatty acid chains. The overall reduction in mature CL species within the brain is consistent with defective remodeling of nascent CL. We have demonstrated that TAZ kd mice exhibited signs of elevated anxiety and dysfunctional recognition memory. The corresponding structural changes in the neuronal layer of hippocampal CA1 neurons and reduced level of synaptic proteins are consistent with attenuated neuronal signaling[47].

Excess mitochondrial ROS production induces oxidative modification of cellular macromolecules, inhibits protein function and promotes cell death. The brain is particularly susceptible to oxidative stress due to high levels of oxidative respiration[57]. We observed a significant increase in ROS production from mitochondria isolated form TAZ kd mouse brain compared to the littermate controls. This is consistent with other reports of elevated ROS production and/or oxidative damage in TAZ-deficiency[34,50,58,59]. In neurons, complex I is considered to be the primary site for ROS formation and its dissociation from supercomplexes promotes excessive production[55,60]. The rate of mitochondrial ROS production may also vary with the concentration of a given electron carrier, overall respiratory rate and level of damage to the respiratory chain[57]. While TAZ-deficiency in the brain did not result in supercomplex dissociation, the elevated basal respiratory activity combined with a significant increase in the “free” monomeric form of complex I provides a basis for excessive ROS. It is established that high levels of mitochondrial ROS and the subsequent oxidative stress can cause cell death via apoptosis or necrosis in the brain[61]. In

mouse brain studies, cognitive dysfunction has correlated with the level of oxidative damage[62]. Interestingly, CAI neurons in the hippocampus, which were significantly deranged in the TAZ kd mouse, are among the most sensitive to oxidative stress[61]. Elevated levels of neuronal ROS and/or peroxidized lipid metabolites may additionally promote microglial activation[57]. Targeting of defective and/or dying neurons by microglial phagocytosis in response to oxidative stress is a potential cause of neuronal loss in major neurodegenerative disorders[57,63–66]. We hypothesize that the elevated microglial activation in TAZ kd brain maybe in response to increased neuronal oxidative stress. Alternatively, microglial activation maybe due to their own aberrant level of ROS. This process however is typically supported by an inflammatory response, which remained similar (GFAP) between the genotypes[61].

We have demonstrated that TAZ-deficiency increases several phospholipid classes in the brain including PE and PC. Interestingly, an increase in mitochondrial PE content in the liver has been correlated with elevated complex IV activity, mitochondrial respiration and ATP production[67]. Dietary supplementation of PS has been consistently demonstrated to improve cognitive function in both experimental animals and humans[68]. The neuronal PC content is also critical for cognitive function. For example, PC biosynthesis is important for membrane synthesis during neuronal differentiation[69]. Thus, the elevation of PE, PS and PC in the brain of TAZ kd mice may reflect an adaptive response to restore cognitive function. Alternatively, the alteration in PL content may be a mechanism to maintain the intrinsic curvature of mitochondrial membranes in CL-deficiency.

In the brain of TAZ kd mice we additionally determined significant alterations in lysophospholipid content. The specific role for each molecular species of lysophospholipids in the brain are only beginning to be elucidated. For example, there is evidence that PUFA-containing LPI is important for cortical lamination and neuronal migration[70,71]. Lysophosphatidylcholine maybe essential in human brain development and function because they provide a preformed phospholipid source for membrane repair and supply essential PUFA species[72,73]. Elevated brain LPS levels, particularly very-long-chain species, results in a neuroinflammatory response that may promote microglial and neurobehavioral abnormalities[74]. Therefore, in the TAZ kd mice, the reduction in LPI and LPC species combined with elevation in LPS species may contribute to the cognitive dysfunction. Our current report provides a basis for future investigations into the roles of brain lysophospholipids.

In summary, our results provide novel information on the phospholipid and pathological changes that occur in the brain of TAZ kd mice. These findings underscore the role of TAZ-mediated CL remodelling in maintaining normal cognitive and mitochondrial function. Furthermore, we have highlighted pathological changes in the hippocampus as a result of altered CL metabolism. Thus, CL content in the brain may be a potential therapeutic target for improving cognitive performance in a variety of neurodegenerative disorders as well as BTHS.

Materials and Methods

Materials

Antibodies used for immunohistochemical analysis were obtained from Abcam (Cambridge, MA, USA) and Santa Cruz Biotechnology Inc. (Dallas, TX, USA). Western blot components were obtained from BioRad (Mississauga, ON, Canada) and GE Healthcare Life Sciences (Mississauga, ON, Canada). Lipid standards were obtained from Avanti Polar Lipids (Alabaster, AL, USA) or Cayman Chemical Co. (Ann Arbor, MI, USA). MLCL was synthesized in house as described[75]. All other biochemical agents, components and drugs were ASC grade and were obtained from either Sigma-Aldrich (St. Louis, MO) or Thermo Fisher Scientific (Carlsbad, CA).

Animals

All protocols were performed with approval of the University of Manitoba Animal Policy and Welfare Committee. Animals were maintained in an environmentally controlled facility (12 h light/dark cycle) with free access to food and water. TazKD mice were generated by mating male mice [B6.CgGt(ROSA)26Sortm1(1H/tetO-RNAi:Taz, Cag-tetR)Bsf/ZkhuJ; The Jackson Laboratory, Bar Harbor, ME] which are transgenic (Tg) for a doxycycline (dox) inducible tafazzin specific short-hairpin RNA (shRNA) with female C57BL/6J mice (The Jackson Laboratory) as previously described[34,41]. The knockdown of TAZ (TAZ kd) was induced *in utero* and maintained postnatally by administering dox (625 mg of dox/kg of chow) as part of the standard rodent chow (Harlan, Rodent diet TD.01306). This study focussed on male offspring as BTHS is an X-linked disease. Male mice positive for the tafazzin shRNA transgene were identified by using PCR[41]. Both male Tg (TAZ kd) and NTg wild-type littermate controls were weaned onto the dox containing diet at 3 weeks of age and maintained until the experimental end-point. Mice at 7–10 months of age were used for all experiments with the exception that 3–4 month animals were used for mitochondrial oxygen consumption rates, supercomplex formation, reactive oxygen species quantitation, ATP quantitation and electron microscopy. Male NTg and Tg mice that did not receive doxycycline *in utero* or postnatally were used as an additional experimental control group (Tg/NTg -dox).

Quantitation of brain lipids

Whole mouse brain was harvested and the lipids were extracted using the Folch method[76]. For phospholipid analysis, samples corresponding to approximately 2.5 nanomol of total phosphate was added with the appropriate internal standards (5 picomoles each of PC(17:0/17:0, PG(17:0/17:0, PI(16:0/16:0), CL(14:0/14:0/14:0/14:0), PS(17:0/17:0), PA(17:0/17:0), PE(17:0/17:0)) and analyzed using LC-MS/MS. LC/MS analysis was performed using a Dionex Ultimate 3000 RSLCnano system coupled on-line to a Q-Exactive hybrid quadrupole-orbitrap mass spectrometer (ThermoFisher Scientific) using a Silica(2) column (Luna 3 μm, 100 Å, 150 × 2 mm (Phenomenex)). A multi-step gradient with solvents A (Hexane Propanol/Water/Triethylamine/Formic acid, 43:57:1:0.5:0.01 v/v containing 10 mM Ammonium acetate) and B (Hexane Propanol/Water/Triethylamine/Formic acid, 43:57:1:0.5:0.01 v/v containing 10 mM Ammonium acetate) was used as follows: 0–15 minutes linear gradient from 10% B to 37% A at 200 μl/min, 15–23 minutes

linear gradient from 37% to 40% B at 200 μl/min, 23–25 minutes linear gradient from 40% to 100% B and at a linear increase in flow rate at 200–225 μl/min, 27 – 47 minutes isocratic at 100% B at 225 μl/min, 47–57 minutes linear gradient from 100% to 10% B with a linear decrease in flow rate from 225 to 200 μl/min then the column was re-equilibrated for 13 minutes with 10% solvent B at 200 μl/min. The mass spectrum was acquired in a data dependent acquisition with a negative ion mode from 0–57 minutes. The spray voltage was set as 3.2 KV with a sheath gas flow rate of 10 orbitary units. The spectrum was recorded at 70000 FWHM resolution between 360 to 1600 m/z range with top 10 ions were selected for fragmentation. HCD fragmentation with 24 NCE was used while the ions were isolated at + 1 mz isolation window. The mass spec data was analysed using the sieve 2.1 software using an in house developed database.

Western blot analysis

Tafazzin protein expression was analyzed by harvesting and homogenizing whole brain. The protein concentration was determined and equal amounts loaded (30 ug/lane) separated by electrophoresis on a 12% SDS-PAGE gel. The proteins were then transferred onto a PVDF membrane (Immobilon, Millipore, Bedford, MA) and blocked with 5% non-fat milk in 0.1% tween-20/TBS before overnight incubation at 4°C with primary antibodies (1/1000). The mouse monoclonal antibody raised against tafazzin (Clone 2G3F7) was a generous gift from Dr. Steven Claypool, John Hopkins University (Baltimore, MD). Expression of TAZ in heart homogenate of non-transgenic animals was determined as an antibody control since the protein is highly expressed in cardiac tissue. Expression of citrate synthase (Abcam) protein was used as a protein loading control. Protein levels of TAZ were quantitated by densitometry and normalized against citrate synthase (n=1–3).

RNA isolation and PCR analysis

Total RNA was isolated from whole mouse brain using the RNeasy lipid tissue kit (Qiagen) according to the manufacturers instructions. First-strand cDNA synthesis was performed using SuperScript™ II (Invitrogen) primed by oligo$(dt)_{12–18}$. PCR was performed using the gene specific primers indicated in Table 1. Amplicons were measured using real-time quantitative PCR using Realplex^2 Mastercycler (eppendorf) and mRNA levels were normalized to TFIIB using a standard curve. The abbreviations for mRNAs are: transcription factor II B (TFIIB); tata-box binding protein (TBP); Tafazzin (TAZ); Protein Tyrosine Phosphatase localized to mitochondrion 1 (PTPMT); Phosphatidylglycerol synthase (PGS); Cardiolipin synthase (CLS);

Thin-Layer Chromatography and Phosphorus assay

Total lipids were extracted from heart or liver homogenates (2 mg protein) and amounts of phosphatidylglycerol (PG) and cardiolipin were determined by phosphorus assay[77] following separation by thin-layer chromatography in a developing solvent of chloroform/methanol/acetic acid/formic acid (99%)/water (150/60/20/6/0.5, v/v).

Mitochondrial Analysis

Mitochondrial H_2O_2 levels was quantitated using Amplex® UltraRed reagent. ATP levels was quantitated using ATP Bioluminescent assay kit (Sigma-Aldrich). Mitochondria supercomplexes (30 μg protein) were separated by blue native-polyacrylamide gel electrophoresis and individual complexes visualized using in-gel activity assays[34]. For Complex I: 5 mM Tris pH 7.4, 0.3 mM β-nicotinamine adenine dinucleotide, 0.1 mM nitrotetrazolium blue. For Complex IV: 50 mM sodium phosphate pH 7.2, 5 mM cytochrome C, 2 mM 3'3'diaminobenzidine. The level of supercomplexes and individual complexes were quantitated by densitometry.

Oxygen consumption rate (OCR) was measured from isolated mouse brain mitochondria (5 μg for Complex I, 10 μg for Complex II) using a Seahorse Bioscience instrument. The base media contained:70 mM sucrose, 220 mM Mannitol, 5 mM KH_2PO_4, 5 mM $MgCl_2$, 2 mM HEPES, 1 mM EGTA, 0.2 % BSA. To assay Complex I the media additionally contained 5 mM malate and 5 mM glutamate. To assay Complex II the media additionally contained 5 mM succinate and 2 uM rotenone. The following reagents were then added in order during the oxygen consumption measurements: 4 mM ADP, 2.5 uM oligomycin, 1 uM (Complex I) or 5 uM FCCP (Complex II), 4 uM antimycin A. State I was considered to be basal respiration prior to the addition of ADP. State III was considered ADP facilitated oxygen consumption. State IIIu was considered FCCP facilitated oxygen consumption. State IV was considered oxygen consumption in the presence of oligomycin. Since the addition of antimycin A inhibits all mitochondrial respiration, any respiration in the presence of antimycin A was subtracted from all OCR values prior to generating average values. All data was normalized to mitochondrial protein content following OCR measurements. The % increase in OCR was calculated using the following formula (State III or State IIIu-State I)/ State I *100.

Transmission electron microscopy

Mice were anesthetized (3–4 months of age) and perfused with 4% formaldehyde and 1.25% glutaraldehyde in phosphate buffered saline (pH 7.5). The brain was removed and the left and right dorsal hippocampus CAI region was dissected between −1.5 and −3 from bregma. Samples were incubated in 5% sucrose in 0.1M Sorensen's buffer (> 24h at 4°C) followed by post-fixation in 1% osmium tetroxide (2h at RT). The samples were then gradually dehydrated with ethanol, followed by 100% methanol and 100% propylene oxide. The solvent was replaced with embedding medium and cured at 60°C for 24 h. Sections were cut on a Reichert ultrathin microtome at a thickness of 70–90mm before being collected on EM grids and stained with UranyLess and lead citrate. The samples were then imaged using a Philips CM10 electron microscope at 46 000X or 64 000x magnification. The following measurements were performed using Image J (NIH): (1) cross-sectional area of mitochondria (average cross-sectional area of mitochondria) (2) mitochondrial shape (average of radius a/radius b) (3) mitochondrial area density (total cross-sectional area of mitochondria/unit area) (4) mitochondrial density (# mitochondria/unit area). For each animal multiple >30 images were generated in multiple randomly selected sections.

Behavioural tests

Mice at seven-months of age were challenged with behavioural tests to analyse motor function, anxiety, attention, exploration, memory and learning abilities. For the Open Field (OF) test mice were placed within a walled arena (white square Plexiglas chamber; L 75 cm × W 75 cm × H 75 cm, illuminated at 8–13 lx red light) for 10 min. Locomotor activity was recorded with a HVS Image 2100 Plus video tracking system software (HVS Image Ltd., Twickenham, Middlesex, UK) for later analysis of general activity level, anxiety, attention, and exploration tendency as previously described[78].

Novel object recognition memory test assessing memory and learning abilities related to hippocampal function was performed as previously described as a continuum of the OF test[79–84]. Two identical objects were placed in the OF arena and mice were allowed to explore the objects freely during a 10 min training session. On the following day, mice were placed back into the OF arena for the 10 min test session, during which they were presented with one of the objects used during training (now considered as a familiar object) and with a novel, unfamiliar object of different shape, texture and transparency. Object locations were kept constant during training and test sessions for all animals. Frequency of object interactions and time spent exploring each object was recorded with a video tracking system. Arenas and objects were cleaned with 70% ethanol between each mouse.

Immunohistochemistry analysis of hippocampus

The brain was dissected and the left hemisphere processed for immunohistochemical evaluation. Immunostaining was performed on 30 μm coronal sections with the primary antibodies anti-NeuN (Chemicon international, 1:500), anti-synaptophysin (Sigma, 1:500), and anti- glial fibrillary acidic protein (GFAP; EMD Millipore, 1:500)[85]. After washing, sections were treated with either Dylight 488 or 594 conjugated anti-IgG (Thermofisher, 1:500) secondary antibodies. Immunofluorescence imaging and semi-quantitative analysis was performed using a Zeiss fluorescent microscope facilitated by an individual blinded for mice genotype. ImageJ program (NIH) was used to accurately measure the hippocampal neuronal CA1 layer thickness. Image J was also used to quantitate synaptophysin, NeuN and GFAP protein expression levels by measuring the mean optical density of the staining intensity in the designated, uniform-sized regions of interest. Neuronal numbers and densities were determined by expression of NeuN, synaptic vesicle density was determined by expression of pre-synaptic vesicle protein, synaptophysin, and astrogliosis was determined by expression of glial fibrillary acidic protein (GFAP). The values were measured on a minimum of three matching hippocampal regions from each mouse. The background values measured for each section were subtracted, and the resulting values were averaged to give one value per mouse.

Microglial activation was determined based on cell number, morphology and expression of ionized calcium-binding adapter molecule-1 (Iba1) as previously described[86]. Briefly, Iba1 immunohistochemistry using the primary antibody anti-Iba1 (Wako, 1:500) was performed on coronal sections as described above and the intensity of staining evaluated using Image J. In addition, an observer blinded by genotype counted both the total number of microglial and the % of those cells with an amoeboid morphology (enlarged soma and thickened

processes) in a defined 200μm X 200μm hippocampal region. Three sections from each animal were evaluated. Microglial activation was then scored 0 (no activation) to 3 (highly activated) based on the level of cell number, % amoeboid morphology and Iba1 intensity as indicated in Table 2.

Statistical analysis

All data were expressed as mean ± SD. Student's t-test was used for statistical analysis or by two-way ANOVA and multiple comparison tests followed by Bonferroni post-hock analysis. A probability value of $p<0.05$ was considered statistically significant.

Acknowledgements

The authors thank Dr. Vernon W. Dolinsky for helpful discussions. Supported by grants from the Children's Hospital Research Institute of Manitoba (GMH, TMK), Heart and Stroke Foundation of Canada (GMH, TMK), Natural Sciences and Engineering Research Council (GMH, TMK), the Barth Syndrome Foundation USA/Canada and (GMH, VEK) Research Manitoba (TMK), US National Institute of Health (AI068021, NS076511, NS061817) (VEK, HB). GMH is the Canada Research Chair in Molecular Cardiolipin Metabolism.

References:

1. White DA, The phospholipid composition of mammalian tissues, in Form and function of phospholipids, Ansell GB, Hawthorne JN, and Dawson RMC, Editors, 1982 Elsevier, Amsterdam, p. 441–461.
2. Hatch GM, Cardiolipin: biosynthesis, remodeling and trafficking in the heart and mammalian cells. International Journal of Molecular Medicine, 1998 1(1): p. 33–41. [PubMed: 9852196]
3. Hauff K, Hatch GM, Cardiolipin metabolism and Barth Syndrome. Progress in Lipid Research, 2006 45(2): p. 91–101. [PubMed: 16442164]
4. Schlame M, Cardiolipin synthesis for the assembly of bacterial and mitochondrial membranes. Journal of Lipid Research, 2008 499(8): p. 1607–1620.
5. Houtkooper RH, Vaz FM, Cardiolipin, the heart of mitochondrial metabolism. Cellular and Molecular Life Sciences, 2008 65(16): p. 2493–2506. [PubMed: 18425414]
6. Hatch GM, Cell biology of cardiac mitochondrial phospholipids. Biochemistry and Cell Biology. 2004 82(1): 99–112. [PubMed: 15052331]
7. Koshkin V, Greenberg M Oxidative phosphorylation in cardiolipin-lacking yeast mitochondria. Biochemical Journal. 2000, 347(3): p. 687–691. [PubMed: 10769171]
8. Koshkin V, Greenberg M Cardiolipin prevents rate-dependent uncoupling and provides osmotic stability in yeast mitochondria. Biochemical Journal. 2002, 364(1): p. 317–322. [PubMed: 11988106]
9. Zhang M, Mileykovskaya E, Dowhan W Gluing the respiratory chain together. Cardiolipin is required for supercomplex formation in the inner mitochondrial membrane. Journal of Biological Chemistry 2002, 277(46): p. 43553–43556. [PubMed: 12364341]
10. Bolhuis PA, Hensels GW, Hulsebos TJ, Baas F, Barth PG (1991) Mapping of the locus for X-linked cardioskeletal myopathy with neutropenia and abnormal mitochondria (Barth syndrome) to Xq28. Amererican Journal of Human Genetics. 1991 48(3): p. 481–485.
11. Adès LC, Gedeon AK, Wilson MJ, Latham M, Partington MW, Mulley JC, Nelson J, Lui K, Sillence DO, Barth syndrome: clinical features and confirmation of gene localisation to distal Xq28. Amererican Journal of Human Genetics, 1993 45(3): p. 327–334.
12. Bione S, D'Adamo P, Maestrini E, Gedeon AK, Bolhuis PA, Toniolo D, A novel X-linked gene, G4.5. is responsible for Barth syndrome. Nature Genetics, 1996 12(4): p. 385–389. [PubMed: 8630491]
13. Xu Y, Malhotra A, Ren M, Schlame M, The enzymatic function of tafazzin. Jouranl of Biological Chemistry, 2006 281(51): p. 39217–39224.

14. Gonzalvez F, Schug ZT, Houtkooper RH, MacKenzie ED, Brooks DG, Wanders RJ, Petit PX, Vaz FM, Gottlieb E, Cardiolipin provides an essential activating platform for caspase-8 on mitochondria. Jouranl of Cell Biology, 2008 183(4): P. 681–696.
15. Ma L, Vaz FM, Gu Z, Wanders RJ, Greenberg ML The human TAZ gene complements mitochondrial dysfunction in the yeast taz1Delta mutant. Implications for Barth syndrome. Journal of Biological Chemistry, 2004 279(43): p. 44394–44399. [PubMed: 15304507]
16. Khuchua Z, Yue Z, Batts L, Strauss AW A zebrafish model of human Barth syndrome reveals the essential role of tafazzin in cardiac development and function. Circulation Research, 2006 99(2): p. 201–208. [PubMed: 16794186]
17. Xu Y, Zhang S, Malhotra A, Edelman-Novemsky I, Ma J, Kruppa A, Cernicica C, Blais S, Neubert TA, Ren M, Schlame M, Characterization of tafazzin splice variants from humans and fruit flies. Journal of Biological Chemistry, 2009, 284(42) : p. 29230–29239. [PubMed: 19700766]
18. Barth PG, Scholte HR, Berden JA, Van der Klei-Van Moorsel JM, Luyt-Houwen IE, Van 't Veer-Korthof ET, Van der Harten JJ, Sobotka-Plojhar MA, An X-linked mitochondrial disease affecting cardiac muscle, skeletal muscle and neutrophil leucocytes. Journal of Neurological Sciences, 1993 62(1–3): p. 327–355.
19. Clarke SL, Bowron A, Gonzalez IL, Groves SJ, Newbury-Ecob R, Clayton N, Martin RP, Tsai-Goodman B, Garratt V, Ashworth M, Bowen VM, McCurdy KR, Damin MK, Spencer CT, Toth MJ, Kelley RI, Steward CG, Barth Syndrome. Orphanet Journal of Rare Diseases, 2013 8: p. 23. [PubMed: 23398819]
20. Pointer CB, Klegeris A Cardiolipin in Central Nervous System Physiology and Pathology. Cellular and Molecular Neurobiology, 2017 37(7): p. 1161–1172. [PubMed: 28039536]
21. Cheng H, Mancuso DJ, Jiang X, Guan S, Yang J, Yang K, Sun G, Gross RW, Han X Shotgun lipidomics reveals the temporally dependent, highly diversified cardiolipin profile in the mammalian brain: temporally coordinated postnatal diversification of cardiolipin molecular species with neuronal remodeling. Biochemistry 2008 47(21): p. 5869–5880. [PubMed: 18454555]
22. Beyer K, Nuscher B Specific cardiolipin binding interferes with labeling of sulfhydryl residues in the adenosine diphosphate/adenosine triphosphate carrier protein from beef heart mitochondria. Biochemistry. 1996 35(49): p. 15784–15790. [PubMed: 8961941]
23. Fry M, Green DE Cardiolipin requirement for electron transfer in complex I and III of the mitochondrial respiratory chain. Journal of Biological Chemistry. 1981 256(4):p. 1874–1880. [PubMed: 6257690]
24. Kagan VE, Bayir HA, Belikova NA, Kapralov O, Tyurina YY, Tyurin VA, Jiang J, Stoyanovsky DA, Wipf P, Kochanek PM, Greenberger JS, Pitt B, Shvedova AA, Borisenko G Cytochrome c/cardiolipin relations in mitochondria: a kiss of death. Free Radicals in Biology and Medicine. 2009 46(11): p. 1439–1453.
25. Gobbi M, Re F, Canovi M, Beeg M, Gregori M, Sesana S, Sonnino S, Brogioli D, Musicanti C, Gasco P, Salmona M, Masserini ME Lipid-based nanoparticles with high binding affinity for amyloid-beta1–42 peptide. Biomaterials 2010 31(25): p. 6519–6529. [PubMed: 20553982]
26. Ghio S, Kamp F, Cauchi R, Giese A, Vassallo N Interaction of α-synuclein with biomembranes in Parkinson's disease--role of cardiolipin. Progress in Lipid Research. 2016 61: p. 73–82. [PubMed: 26703192]
27. Wang Y, Cella M, Mallinson K, Ulrich JD, Young KL, Robinette ML, Gilfillan S, Krishnan GM, Sudhakar S, Zinselmeyer BH, Holtzman DM, Cirrito JR, Colonna M TREM2 lipid sensing sustains the microglial response in an Alzheimer's disease model. Cell. 2015 160(6): p. 1061–1071. [PubMed: 25728668]
28. Christodoulou J, McInnes RR, Jay V, Wilson G, Becker LE, Lehotay DC, Platt BA, Bridge PJ, Robinson BH, Clarke JT, Barth syndrome: clinical observations and genetic linkage studies. American Journal of Medical Genetics, 1994 50(3): p. 255–264. [PubMed: 8042670]
29. Mazzocco MM, Kelley RI, Preliminary evidence for a cognitive phenotype in Barth syndrome. American Journal of Medical Genetics, 2001 102(4): p. 372–378. [PubMed: 11503166]
30. Mazzocco MM, Henry AE, Kelly RI, Barth syndrome is associated with a cognitive phenotype. Journal of Developmental and Behavioral Pediatrics, 2007 28(1): p. 22–30. [PubMed: 17353728]

31. Raches D, Mazzocco MM Emergence and nature of mathematical difficulties in young children with Barth syndrome. Journal of Developmental and Behavioral Pediatrics, 2012 33(4): p. 328–335. [PubMed: 22566029]
32. Ferreira C, Thompson R, Vernon H, Barth Syndrome In: Pagon RA, Adam MP, Ardinger HH, Wallace SE, Amemiya A, Bean LJH, Bird TD, Fong CT, Mefford HC, Smith RJH, Stephens K, editors. 2014 GeneReviews® [Internet]. Seattle (WA): University of Washington, Seattle; 1993–2016.
33. Moser EI, Kropff E, Moser MB, Place cells, grid cells, and the brain's spatial representation system, 2008 31: p. 69–89.
34. Cole LK, Mejia EM, Vandel M, Sparagna GC, Claypool SM, Dyck-Chan L, Klein J, Hatch GM, Impaired Cardiolipin Biosynthesis Prevents Hepatic Steatosis and Diet-Induced Obesity. Diabetes, 2016 65(11): p. 3289–3300, [PubMed: 27495222]
35. Baile MG, Sathappa M, Lu Y-W, Pryce E, Whited K, McCaffery JM, Han X, Alder NN, Claypool SM, Unmodeled and Remodeled Cardiolipin are Functionally Indistinguishable in Yeast. Journal of Biol. Chem, 2014 289(3):p.1768–1778. [PubMed: 24285538]
36. Vreken P, Valianpour F, Nijtmans LG, Grivell LA, Plecko B, Wanders RJ, Barth PG, Defective remodeling of cardiolipin and phosphatidylglycerol in Barth syndrome. Biochemical and Biophysical Research Communications, 2000 279(2): p. 378–382. [PubMed: 11118295]
37. Schlame M, Shanske S, Doty S, König T, Sculco T, DiMauro S, Blanck TJ, Microanalysis of cardiolipin in small biopsies including skeletal muscle from patients with mitochondrial disease. Journal of Lipid Research, 1999 40(9): p. 1585–1592. [PubMed: 10484605]
38. Schlame M, Towbin JA, Heerdt PM, Jehle R, DiMauro S, Blanck TJ, Deficiency of tetralinoleoyl-cardiolipin in Barth syndrome. Annals of Neurology, 2002 51(5): p. 634–637. [PubMed: 12112112]
39. Vartak R, Porras CA-M, Bai Y, Respiratory Supercomplexes: Structure, Function and Assembley. Protein Cell, 2013 4(8):p.582–590. [PubMed: 23828195]
40. Buck K, Walter NAR, Denmark DL, Genetic Variability of Respiratory Complex Abundance, Organization and Activity in Mouse Brain. Genes Brain Behav, 2014 13(2):p.135–143. [PubMed: 24164700]
41. Acehan D, Vaz F, Houtkooper RH, James J, Moore V, Tokunaga C, Kulik W, Wansapura J, Toth MJ, Strauss A, Khuchua Z, Cardiac and skeletal muscle defects in a mouse model of human Barth syndrome. Journal of Biological Chemistry, 2011 286(2): p. 899–908. [PubMed: 21068380]
42. Soustek MS, Falk DJ, Mah CS, Toth MJ, Schlame M, Lewin AS, Byrne BJ, Characterization of a Transgenic Short Hairpin RNA-Induced Murine Model of Tafazzin Deficiency. Human Gene Therapy, 2011 22:p.865–871. [PubMed: 21091282]
43. Phoon CKL, Acehan D, Schlame M, Stokes DL, Yu D, Xu Y, Viswanathan N, Ren M, Tafazzin Knockdown in Mice Leads to a Developmental Cardiomyopathy With Early Diastolic Dysfunction Preceding Myocardial Noncompaction. J. Am. Heart Assoc, 2012 1: p.1–15. [PubMed: 23130111]
44. Bissler JJ, Tsoras M, Goring HHH, Hug P, Chuck G, Tombragel E, McGraw C, Schlotman J, Ralston MA, Hug G, Infantile Dilated X-linked Cardiomyopathy, G4.5 Mutations, Altered Lipids, and Ultrastructural Malformations of Mitochondria in Heart, Liver, and Skeletal Muscle. Laboratory Investigation, 2002 82(3):p.335–344. [PubMed: 11896212]
45. Lehtimäki KA, Peltola J, Liimatainen S, Haapala AM, Arvio M, Cardiolipin and β_2-Glycoprotein I antibodies associate with cognitive impairment and seizure frequency in developmental disorders. Seizure, 2011 20(6): p. 438–441. [PubMed: 21377902]
46. Monteiro-Cardoso VF, Oliveira MM, Melo T, Domingues MR, Moreira PI, Ferreiro E, Peixoto F, Videira RA. Cardiolipin profile changes are associated to the early synaptic mitochondrial dysfunction in Alzheimer's disease. Journal of Alzheimers Disease. 2015, 43(4): p. 1375–1392.
47. Khacho M, Slack RS, Mitochondrial dynamics in the regulation of neurogenesis: From development to the adult brain. Developmental Dynamics, 2018, 247(1): p. 47–53. [PubMed: 28643345]
48. Powers C, Huang Y, Strauss A, Khuchua Z, Dimished Exercise Capacity and Mitochondrial bc1 Complex Deficiency in Tafazzin-knockout Mice. Frontiers in Physiology, 2013 4(74):p.1–8. [PubMed: 23372552]

49. Wang G, McCain M, Yang L, He A, Pasqualini FS, Agarwal A, Yuan H, Jiang D, Zhang D, Zangi L, Geva J, Roberts AE, Ma Q, Ding J, Chen J, Wang D, Li K, Wang J, Wanders RJA, Kulik W, Vaz FM, Laflamme MA, Murry CE, Chien KR, Kelley RI, Church GM, Parker KK, Pu WT, Modeling the Mitochondrial Cardiomyopathy of Barth Syndrome with Induced Pluripotent Stem Cell and Heart-on-Chip Technologies. Nature Medicine, 2014 20(6):p.616–626.
50. Mejia EM, Zegallai H, Bouchard ED, Vanerji V, Ravandi A, Hatch GM, Expression of Human Monolysocardiolipin Acyltransferase-1 Improves Mitochondrial Function in Barth Syndrome Lymphoblasts. J. Biol. Chem, 2018, 293(20):p.7564–7577. [PubMed: 29563154]
51. Sullivan EM, Fix A, Crouch MJ, Sparagna GC, Zecqycki TN, Brown DA, Shaikh SR, Murine Diet-induced Obesity Remodels Cardiac and Liver Mitochondrial Phospholipid Acyl Chains with Differential Effects on Respiratory Enzyme Activity. Journal of Nutritional Biochemistry, 201745:p.94–103. [PubMed: 28437736]
52. Ye C, Lou W, Li Y, Chatzispyrou IA, Huttemann M, Lee I, Hourkooper RH, Vaz FM, Chen S, Greenberg ML, Deletion of the Cardiolpin-Specifc Phospholipase Cld1 Rescues Growth and Life Span Defects in the Tafazzin Mutant: IMPLICATIONS FOR BARTH SYNDROME. J. Bio. Chem, 2014289:p.3114–3125. [PubMed: 24318983]
53. Mulligan CM, Le CH, deMooy AB, Nelson CB, Chicco AJ, Inhibition of Delta-6 Desaturase Reverses Cardiolipin Remodeling and Prevents Contractile Dysfunction in the Aged Mouse Heart Without Altering Mitochondrial Respiratory Function. Journals of Gerontology: Biological Sciences, 2013 69(7):p.799–809.
54. Xu Y, Phoon CKL, Berno B, D'Souza K, Hoedt E, Zhang G, Neubert TA, Epand RM, Ren M, Schlame M, Loss of Protein Association Causes Cardiolipin Degradation in Barth Syndrome. Nat. Chem. Biol, 2016 12(8):p.641–647. [PubMed: 27348092]
55. Lopez-Fabuel I, Douce JL, Logan A, James AM, Bonvento G, Murphy MP, Almeida A, Bolaños JP, Complex I Assembly into Supercomplexes Determines Differential Mitochondrial ROS Production in Neurons and Astrocytes. Proc.Natl.Acad.U.S.A, 2016113(46):p.13063–13068.
56. Mancuso DJ, Kotzbauer P, Wozniak DF, Sims HF, Jenkins CM, Guan S, Han X, Yang K, Sun G, Malik I, Conyers S, Green KG, Schmidt RE, Gross RW Genetic ablation of calcium-independent phospholipase A2{gamma} leads to alterations in hippocampal cardiolipin content and molecular species distribution, mitochondrial degeneration, autophagy, and cognitive dysfunction. Journal of Biological Chemistry, 2009 284(51): p. 35632–35644. [PubMed: 19840936]
57. Colbey JN, Fiorello ML, Bailey DM, 13 Reasons Why the Brain is Susceptible to Oxidative Stress. Redox Biology, 2018 15:p:490–503. [PubMed: 29413961]
58. Chen S, He Q, Greenberg ML, Loss of Tafazzin in Yeast Leads to Increased Oxidative Stress During Respiratory Growth. Mol. Microbiol, 2008 68(4):p.1061–1072. [PubMed: 18430085]
59. Dudek J, Cheng, Balleininger M, Vaz FM, Streckfuss-Bomeke K, Hubscher D, Vukotic M, Wanders RJA, Rehling P, Guan K, Cardilipin Deficiiency Affects Respiratory Chain Function and Organization in an Induced Pluripotent Stem cell Model of Barth Syndrome. Stem Cell Research, 2013 11:p.806–819. [PubMed: 23792436]
60. Bharath MMS, Post-Translational Oxidative Modifications of Mitochondrial Complex I(NADH:Ubiquinone Oxidoreductase): Implications for Pathogenesis and Therapeutics in Human Diseases. Journal of Alzheimer's Disease, 2017 60:p.S69–S86.
61. Stephanatos R, Sanz A, The Role of Mitochondrial ROS in the Aging Brain. FEBS Letters, 2018 592:p.743–758. [PubMed: 29106705]
62. Forster JJ, Dubey A, Dawson KM, Stutts WA, Lai H, Sohal RS Age-related Losses of Cognitive Function and Motor Skills in Mice are Associated with Oxidative Protein Damage in the Brain. Proc Natl. Acad. U.S.A, 199693(10):p.4765–4769.
63. Angelova PR, Abramov AY, Role of Mitochondrial ROS in the Brain: From Physiology to Neurodegeneration. FEBS Letters, 2018 592:p.692–702. [PubMed: 29292494]
64. Hughes V, Microglia: *The constant gardeners*. Nature, 2012 485(7400): p. 570–572. [PubMed: 22660301]
65. Paolicelli RC, Bolasco G, Pagani F, Maggi L, Scianni M, Panzanelli P, Giustetto M, Ferreira TA, Guiducci E, Dumas L, Ragozzino D, and Gross CT Synaptic pruning by microglia is necessary for normal brain development. Science, 2011 333(6048): p. 1456–1458. [PubMed: 21778362]

66. Wu Y, Dissing-Olesen L, MacVicar BA, Stevens B, Microglia: Dynamic Mediators of Synapse Development and Plasticity. Trends in Immunology, 2015 36(10): p. 605–613. [PubMed: 26431938]

67. Ball WB, Neff JK, Gohil VM, The Role of Nonbilayer Phospholipids in Mitochondrial Structure and Function. FEBS Letters. 2018 592(8):p.1273–1290. [PubMed: 29067684]

68. Kim H, Huang BX, Spector AA, Phosphatidylserine in the Brain: Metabolism and Function, Progress in Lipid Research, 2014 56:p.1–18. [PubMed: 24992464]

69. Paoletti L, Elena C, Domizi P, Banchio C, Role of Phosphatidylcholine During Neuronal Differentiation. IUBMB Life, 2011 (63):p.714–720. [PubMed: 21818839]

70. Deliu E, Sperow M, Console-Bram L, Carter RL, Tilley DG, Kalamarides DJ, Kirby LG, Brailoiu C, Brailoiu E, Benamar K, Abood ME, The lysophosphatidylinositol Receptor GPR55 Modulates Pain Perception in the Periaqueductal Gray. Molecular Pharmacology, 2015 88(2):p.265–272. [PubMed: 25972448]

71. Lee H-C, Inoue T, Sasaki J, Kubo T, Matsuda S, Nakasaki Y, Mattori M, Tanaka F, Udagawa O, Kono N, Itoh T, Ogiso H, Taguchi R, Arita M, Sasaki T, Arai H, LPIAT1 Regulates Arachidonic acid content in Phosphatidylinositol and is required for Cortical Lamination in Mice. Molecular Biology of the Cell, 2012 24:p.4689–4700.

72. Alakbarzade V, Hameed A, Quek DQY, Chioza BA, Baple EL, Cazenave-Gazziot A, Nguyen LN, Wenk MR, Ahmad AQ, Sreekantan-Nair AS, Weedon MN, Rich P, Patton MA, Warner TT, Silver DL, Crosby AH, A Partially Inactivating Mutation in the Sodium-Dependent Lysophosphatidylcholine Transporter MFSD2A causes a Non-lethal Microcephaly Syndrome. Nature Genetics, 2015 47(7):p.814–818. [PubMed: 26005865]

73. Bluxztajn JK, Slack BE, Mellott TJ, Neuroprotective Actions of Dietary Choline. Nutrients, 2017 9(8):pii. E815. [PubMed: 28788094]

74. Blankman JL, Long JZ, Trauger S,A, Siuzdak G, Cravatt BF, ABHD12 Controls Brain Lysophosphatidylserine Pathways that are Deregulated in a Murine Model of the Neurodegenerative Disease PHARC. Proc. Natl. Acad. U.S.A, 2013 110(4):p.1500–1505.

75. Tyurina YY, Poloyac SM, Tyurin A, Kapralov AA, Jiang J, Anthonymuthu TS, Kapralova VI, Vikulina AS, Jung MY, Epperly MW, Mohammadyani D, Klein-Seetharaman J, Jackson TC, Kochanek PM, Pitt BR, Greenberger JS, Vladimirov YA, Bayır H, Kagan VE A mitochondrial pathway for biosynthesis of lipid mediators. Nature Chemistry, 2014 6(6): p. 542–552.

76. Folch J, Complete fractionation of brain cephalin; isolation from it of phosphatidyl serine, phosphatidyl ethanolamine, and diphosphoinositide. Journal of Biological Chemistry, 1949 177(2): p. 497–504. [PubMed: 18110427]

77. Bartlett GR, Colorimeter Assay Methods for Free and Phosphorylated Glyceric Acids., J. Biol. Chem, 1959 186(2):p.469–471.

78. Gould TD, Dao DT, Kovacsics CE The Open Field Test In, Mood and Anxiety Related Phenotypes in Mice. Gould T, Editor. Neuromethods, 2009 42 Humana Press, Totowa, NJ.

79. Moses SN, Cole C, Driscoll I, Ryan JD, Differential contributions of hippocampus, amygdala and perirhinal cortex to recognition of novel objects, contextual stimuli and stimulus relationships. Brain Research Bulletin, 2005 67(1–2): p. 62–76. [PubMed: 16140164]

80. Cohen SJ, Stackman RW Jr., Assessing rodent hippocampal involvement in the novel object recognition task. A review. Behavorial Brain Research, 2015 285: p. 105–117.

81. Wakade C, Sukumari-Ramesh S, Laird MD, Dhandapani KM, and Vender JR, Delayed reduction in hippocampal postsynaptic density protein-95 expression temporally correlates with cognitive dysfunction following controlled cortical impact in mice. Journal of Neurosurgery, 2010 113(6): p. 1195–1201. [PubMed: 20397893]

82. Stackman RW Jr., Cohen SJ, Lora JC, Rios LM, Temporary inactivation reveals that the CA1 region of the mouse dorsal hippocampus plays an equivalent role in the retrieval of long-term object memory and spatial memory. Neurobiol. Learn. Memory, 2016 133: p. 118–128.

83. Kinnavane L, Amin E, Olarte-Sanchez CM, Aggleton JP, Detecting and discriminating novel objects: The impact of perirhinal cortex disconnection on hippocampal activity patterns. Hippocampus, 2016 26(11): p. 1393–1413 [PubMed: 27398938]

84. Kauppinen TM, Suh SW, Higashi Y, Berman AE, Escartin C, Won SJ, Wang C, Cho SH, Gan L, Swanson RA, Poly(ADP-ribose)polymerase-1 modulates microglial responses to amyloid beta. Journal of Neuroinflammation, 2011 8: p. 152. [PubMed: 22051244]

85. Vuong B, Odero G, Rozbacher S, Stevenson M, Kereliuk SM, Pereira TJ, Dolinsky VW, Kauppinen TM Exposure to gestational diabetes mellitus induces neuroinflammation, derangement of hippocampal neurons, and cognitive changes in rat offspring. Journal of Neuroinflammation, 2017 14(1): p. 80. [PubMed: 28388927]

86. Won SJ, Kim JH, Yoo BH, Sohn M, Kauppinen TM, Park MS, Kwon HJ, Liu J, Suh SW Prevention of hypoglycemia-induced neuronal death by minocycline. Journal of Neuroinflammation, 2012 9: p. 225. [PubMed: 22998689]

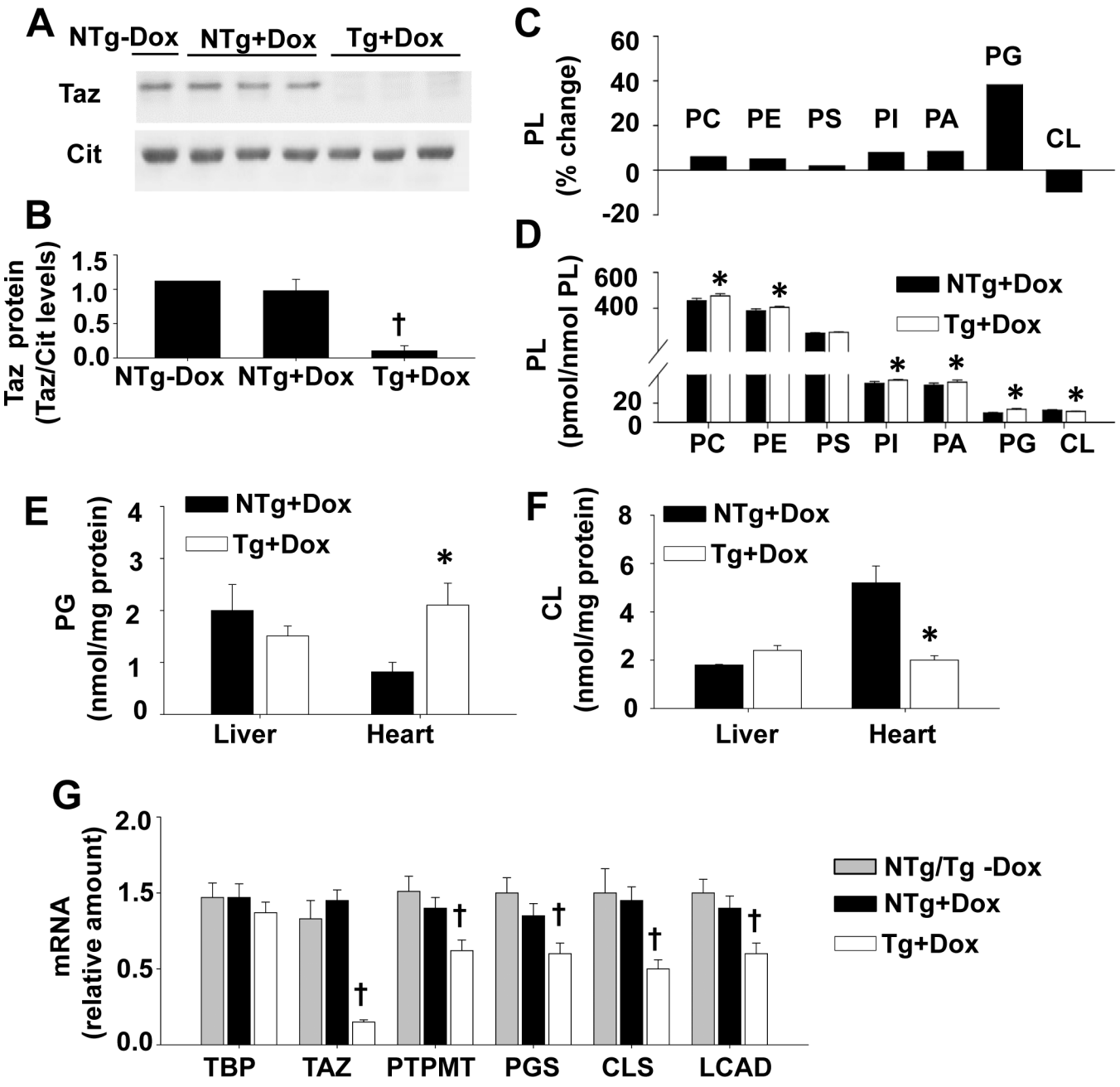

Figure 1.

Tafazzin protein and total CL levels are reduced in TAZ kd mice.

A: Dox-inducible knockdown of TAZ protein was determined by immunoblot using heart isolated mitochondrial (12.5 μg) or total brain homogenates (30 μg). Citrate synthase (Cit) was used as the protein loading control. (B) Protein levels of TAZ were quantitated by densitometry and normalized against citrate synthase (n=1–3). Liquid chromatography-mass spectrometry was used to quantitate phospholipid amounts in whole brain (n=8). Total phospholipid values are expressed as a % change in the TAZ kd mice (Tg +dox) compared to the littermate (NTg +dox) controls [((NTg+dox) – (Tg+dox))/(NTg +dox)x100](C) or pmol/nmol total PL (D). Phosphatidylglycerol (E) and cardiolipin (F) content was measured

in liver and heart homogenates by phosphorus assay (n=3). (G) mRNA levels of the indicated genes were measured by qPCR and normalized to TFIIB (n=11–13). Data are means ±SD. *$p<0.05$ compared with NTg +dox mice. †$p<0.05$ Tg +dox compared to all other groups.

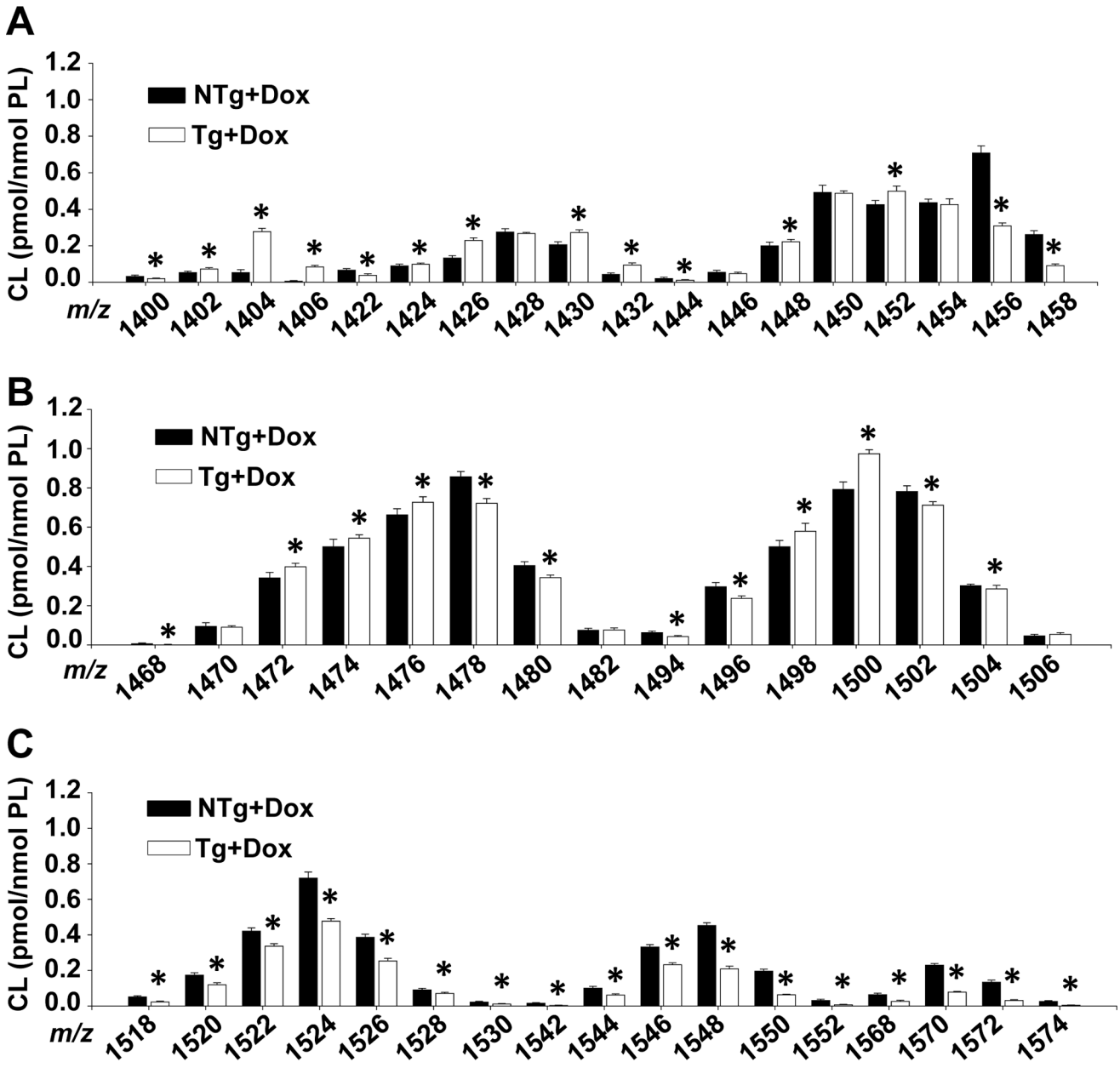

Figure 2.

Brain cardiolipin species are altered in TAZ kd mice.

Liquid chromatography-mass spectrometry was used to quantitate lysophospholipid amounts in whole brain. Individual CL species are arranged by mass (*m/z*) (A-C) Data are means ±SD. **p*<0.05 compared with NTg +dox mice.

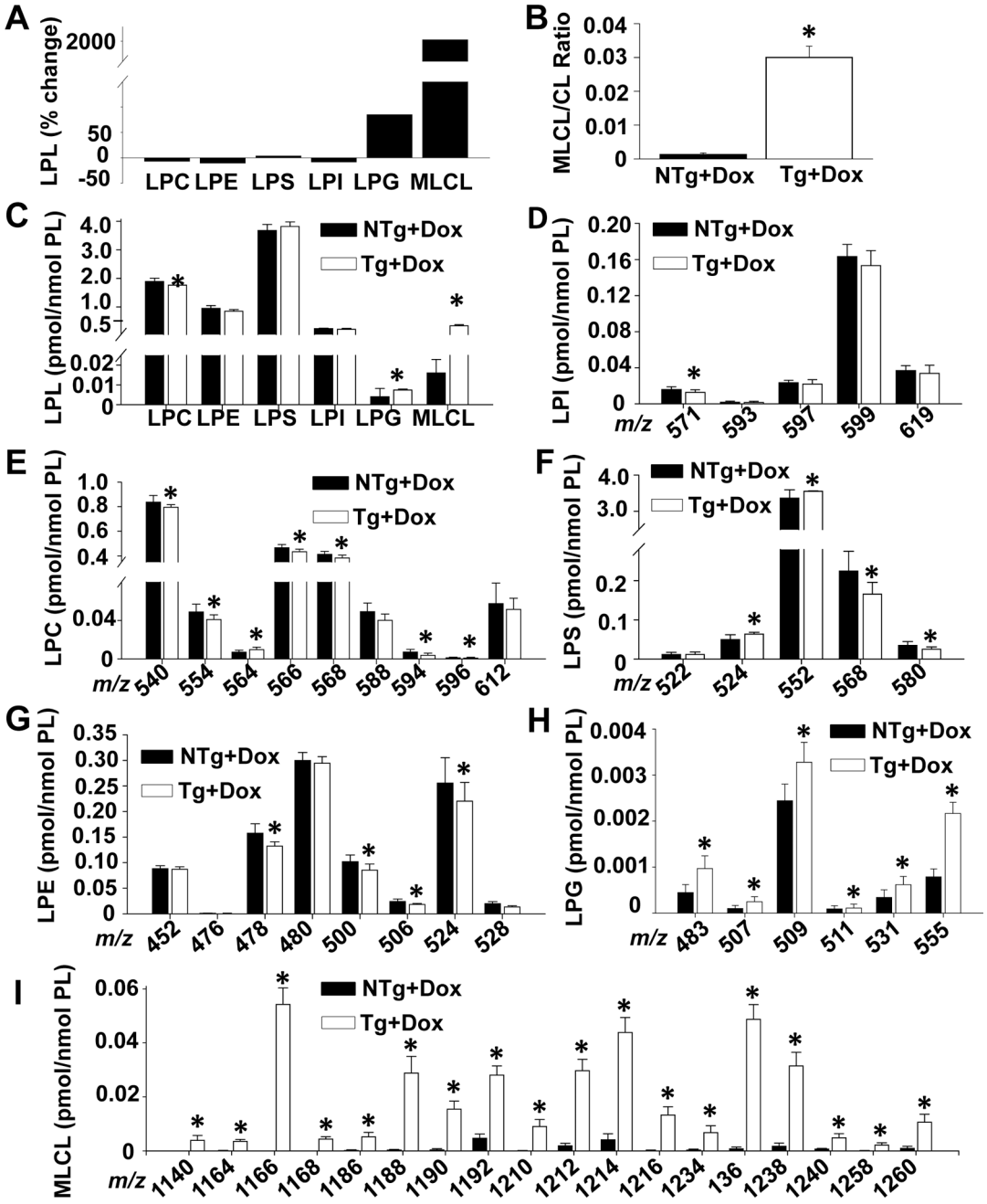

Figure 3.

Brain lysophospholipid levels are altered in TAZ kd mice.

Liquid chromatography-mass spectrometry was used to quantitate lysophospholipid amounts in whole brain. Total lysophospholipid values are expressed as a % change in the Taz kd mice (Tg +dox) compared to the littermate (NTg +dox) controls [((NTg+dox) – (Tg+dox))/(NTg +dox)x100] (A), as a ratio of total MLCL/total CL (B) or pmol/nmol total PL (C). Individual lysophospholipid species were quantitated and arranged by mass (*m/z*) for LPI (D), LPC (E), LPS (F), LPE (G), LPG (H) and MLCL (I). Data are means ±SD (n=8). **p*<0.05 compared with NTg +dox mice. †*p*<0.05 Tg +dox compared to all other groups.

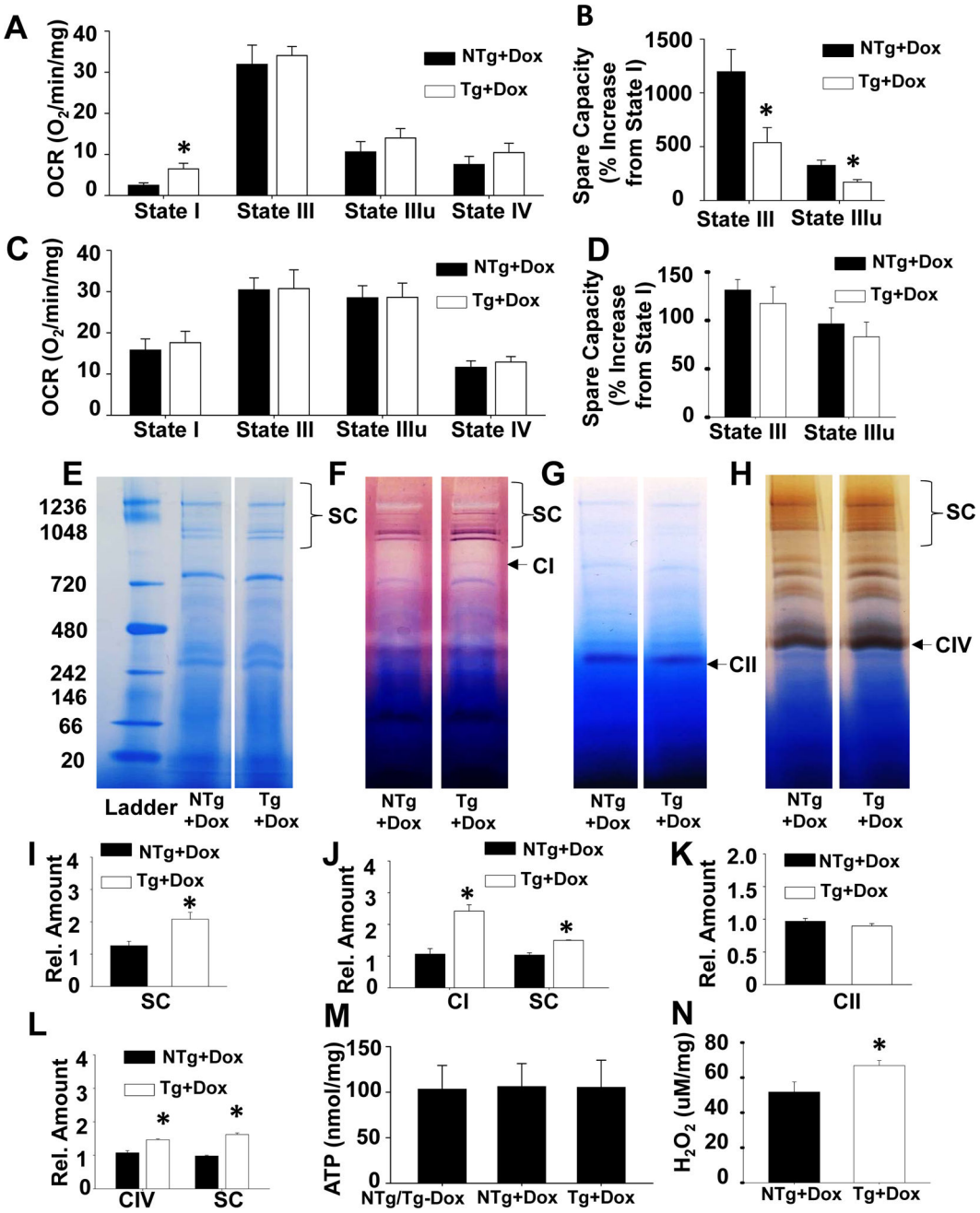

Figure 4.

Altered mitochondria organization and function in TAZ kd mouse brain.

Oxygen consumption rate (OCR) was measured from isolated mouse brain mitochondria for Complex I in several respiration states (A) and % increase in OCR from state I calculated (B) using a Seahorse Bioscience instrument. Oxygen consumption was also measured for Complex II in various respiration states (C) and % increase in OCR calculated (D). All data was normalized to mitochondrial protein content following OCR measurements (n=4–6). The % increase in OCR was calculated using the following formula (State III or State IIIu-State I)/State I *100. Supercomplexes were separated by blue native PAGE (E) prior to

conducing in-gel activity assays for mitochondrial complexes I (F), II, (G) and IV (H) The location of each individual complex is indicated as CI, CII or CIV respectively. The supercomplexes which contain the complex of interest (i.e. active complex) are indicated with brackets at the top of each gel. The ladder size is indicated in kDa on the left and each lane is representative of 3 animals per group. Densitometry analysis of BNpage (I), Complex I (J), Complex II (K) and Complex IV (L) was conducted on the visualized supercomplexes and/or the free individual complex as indicated. Quantitation of ATP content of whole brain homogenate (M) and H202 production from isolated brain mitochondria (N). Data are means ±SD (n=5–6). *p<0.05 compared with NTg +dox mice

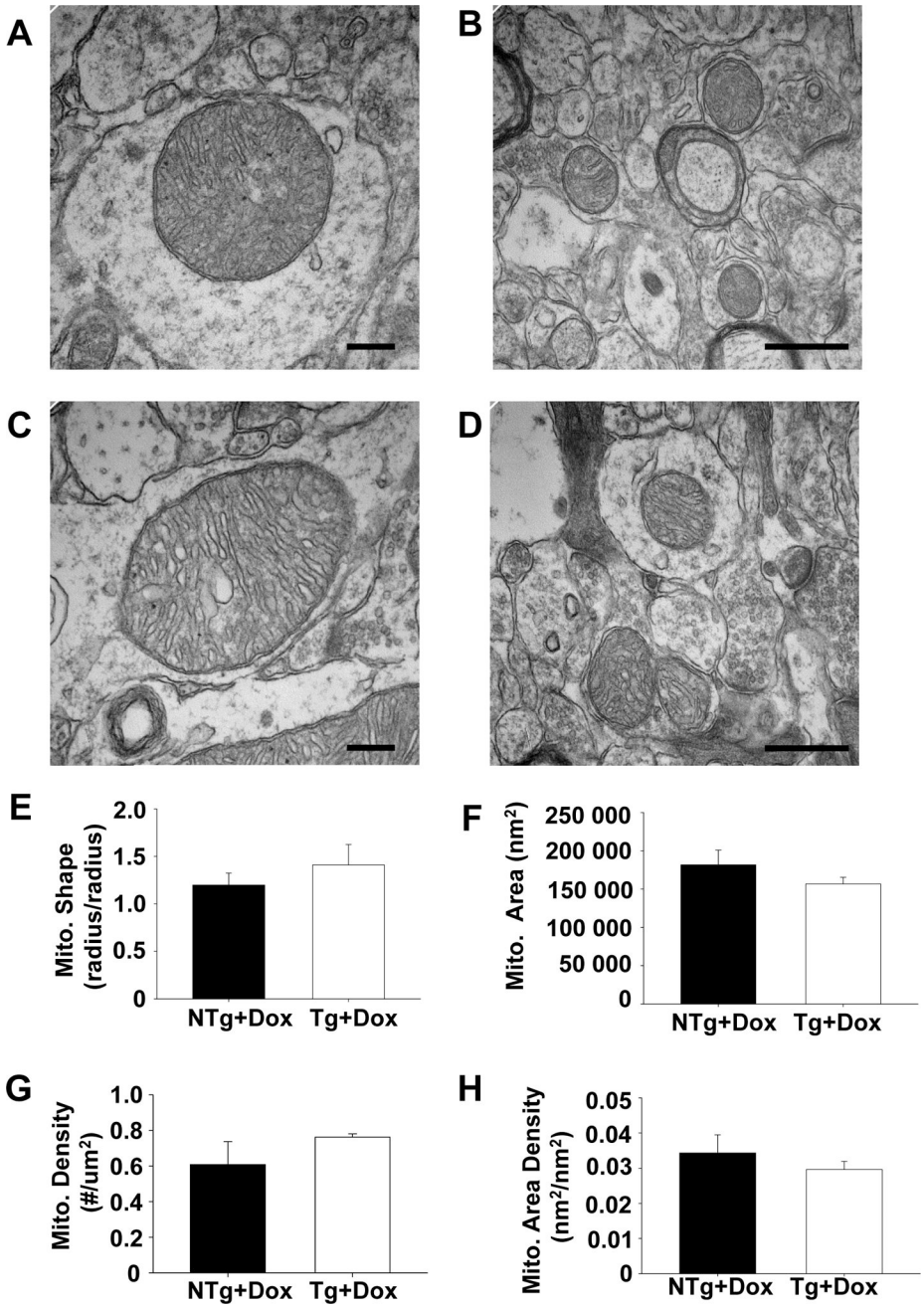

Figure 5.

Mitochondria maintained normal morphology in the brain of TAZ kd mice.

Representative electron micrographs of mitochondria in the dorsal hippocampal CAI region of NTg+dox (A,B) and TAZ-deficient mice (Tg+dox) (C,D). Morphometric analysis of mitochondria were performed to measure mitochondrial shape (E), cross-sectional area (F), and mitochondrial density (G,H). Data are means ±SD (n=2 animals). The scale bars are 200 μm for A,C and 500 μm for B,D.

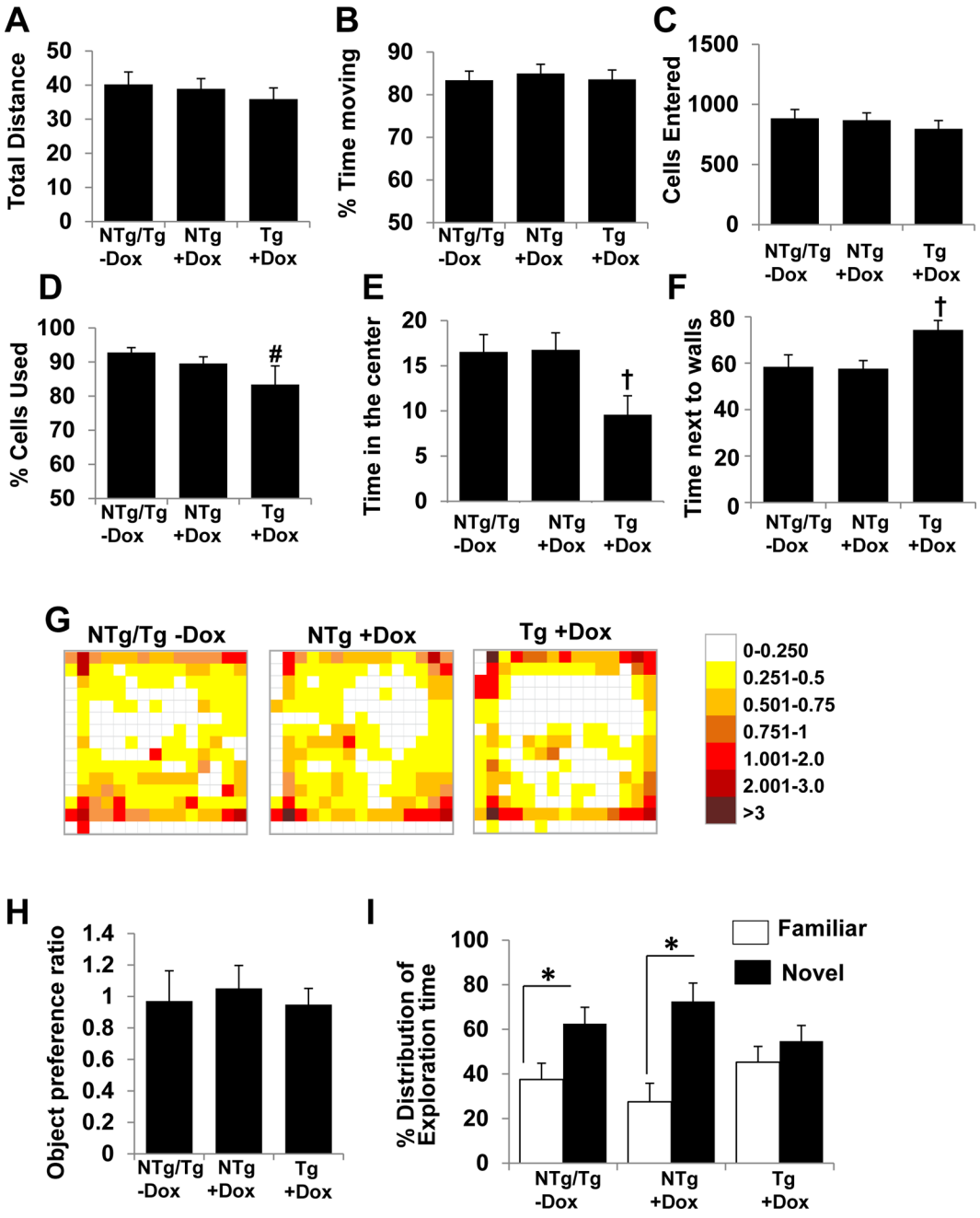

Figure 6.

TAZ kd mice exhibit normal motor functions with signs of increased anxiety and impaired memory.

The motor functions were analyzed during a 15 min open field test based on total distance travelled in meters (A), % time moving (B), number of cells entered (C) and % of cells used (D). Anxiety was analyzed via a heat map (G) and is based on the % time spent in the center (E) and the % time spent next to the walls (F) of the open field. Memory and learning abilities of the animals was assessed by Novel Object Recognition test. (H) Object preference ratio during the initial training calculated as time spent between two identical

objects. (I) % distribution of exploration time between familiar and novel objects after the initial training. Data are means ±SD (n=7). *p<0.05 Tg +dox compared with NTg +dox mice. †p<0.05 Tg +dox compared to all other groups. #p<0.05 compared with NTg/Tg-dox mice.

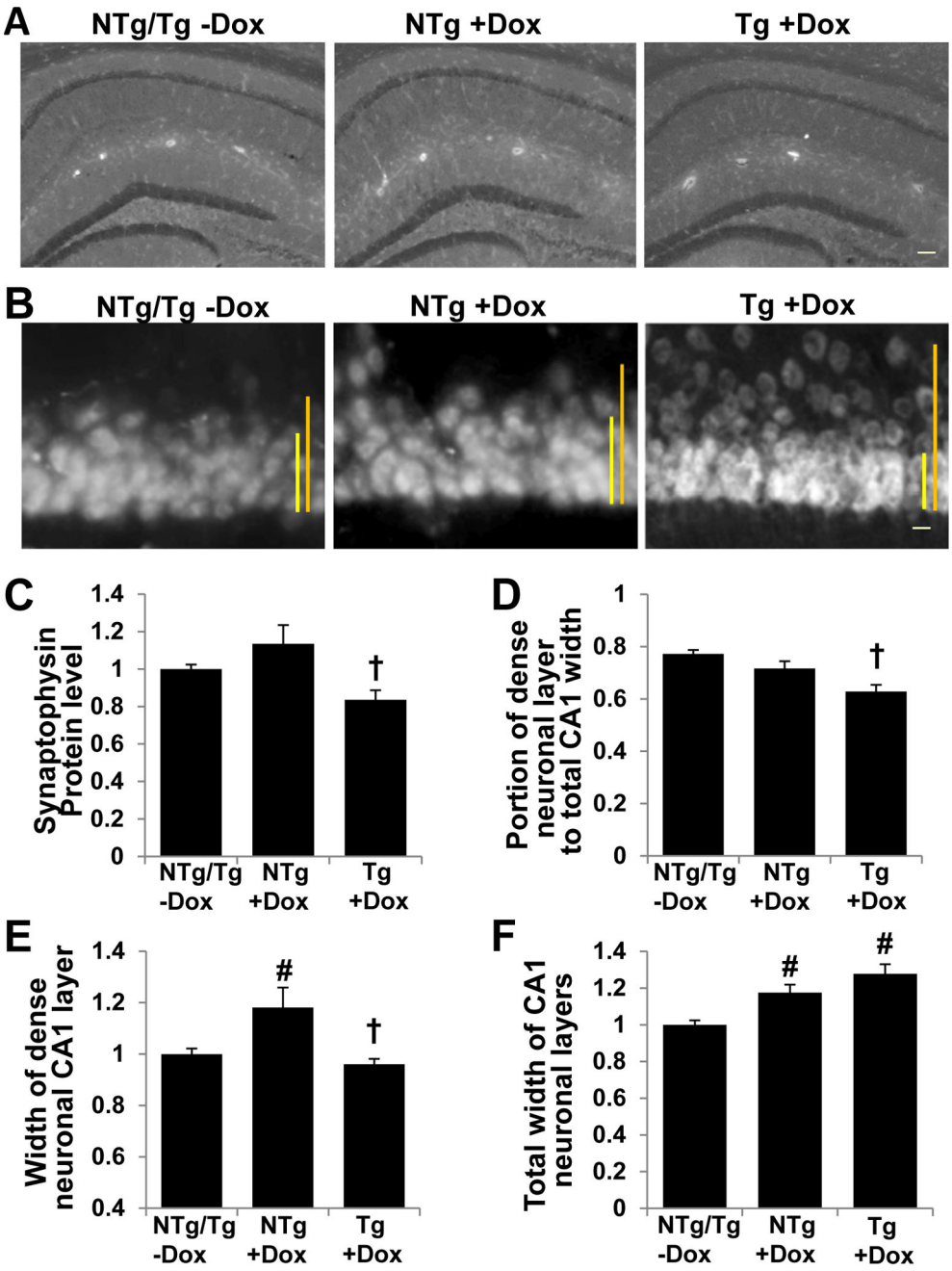

Figure 7.

TAZ kd brain exhibits reduced synaptophysin protein expression and structural changes in hippocampal CA1 neurons.

The left hemisphere of the brain was processed and synaptophysin protein detected (A) and quantitated (C) for each mouse genotype. NeuN protein was detected demonstrating derangement of neurons at the CA1 layer (B), the size of the densely organized CA1 neuronal region (E: yellow bar in B), the total width of the CA1 neuronal layer (F; orange bar in B), and the ratio between the width of densely organized neuronal region and the total width of the CA1 layer (D). Data in C, E and F are expressed relative to Ntg/Tg-Dox. Data

are means ±SD (n=7). †p<0.05 Tg +dox compared to all other groups. #p<0.05 compared with NTg/Tg -dox mice. The scale bars are 100 μm for A and 10 μm for B.

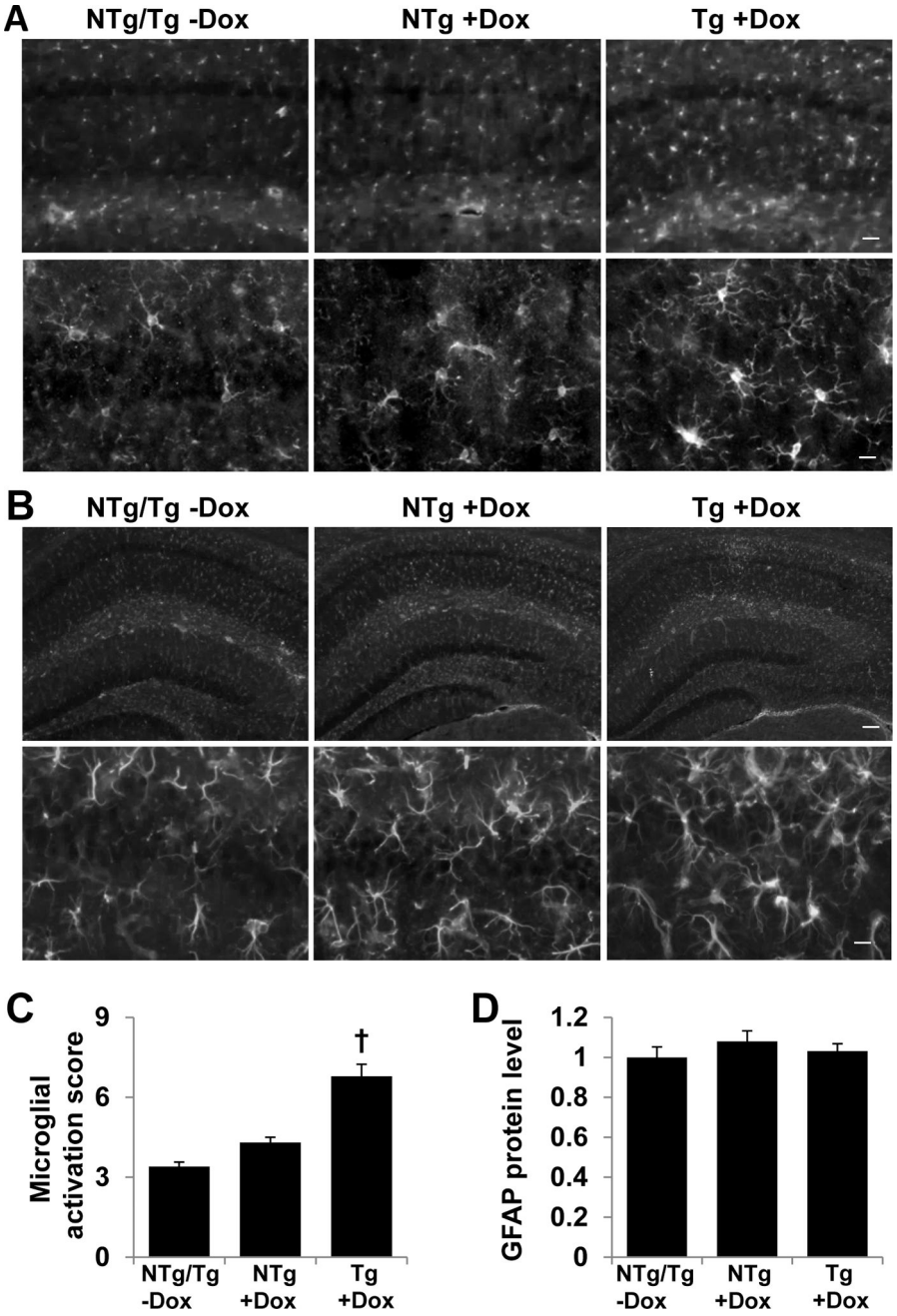

Figure 8.

TAZ kd brain exhibits elevated microglial activation.

The left hemisphere of the brain was processed and microglial morphology determined via Iba-1 protein content (A) and a microglial activation score provided (C) for each mouse genotype. Reactive astrogliosis was determined via GFAP protein content (B) and was quantitated (D). Data in C and D are expressed relative to Ntg/Tg-Dox. Data are means ±SD (n=7). †p<0.05 Tg +dox compared to all other groups. The scale bars are 50μm (A, upper panel), 10μm (A, lower panel), 100μm (B, upper panel) and 10μm (B, lower panel).

Table 1:

PCR primer sequences

Gene	Forward Sequence	Reverse Sequence
TfIIb	TGGAGATTTGTCCACCATGA	GAATTGCCAAACTCATCAAAACT
Tbp	ACCCTTCACCAATGACTCCTATG	TGACTGCAGCAAATCGCTTGG
Taz	GACCCTCATCTCTGGGGGAT	CAGCTCCTTGGTGAAGCAGA
Ptpmt	GCAACACCTCGAAGGAATGG	GAGATTGGCCAAGGTTGGGA
Pgs	ACACAGGTTCCAGTGGATCAG	TTTATCTGCCCCTTCATGAGC
Cls	GAGCTGTCCATACGGCCTC	GGATTTTCATACGAGCTGGCG
Lcad	GCGAAATACTGGGCATCTGAA	TCCGTGGAGTTGCACACATT

Table 2.

Criteria for evaluating microglial activation status.

Score	Ibal expression	Morphology
0	0 microglial with expression	No microglial with activated ameboid shape
1	1–19 microglial with expression	1–40% of Ibal positive microglial with ameboid shape
2	20–39 microglial with expression	40–90% of Ibal positive microglial with ameboid shape
3	>40 microglial with expression	>90% of Ibal positive microglial with ameboid shape